Thermal Spray Coatings Engineered from Nanostructured Ceramic Agglomerated Powders for Structural, Thermal Barrier and Biomedical Applications

Lima, R. S.; Marple, B. R.

Publisher's version / la version de l'éditeur:
Journal of Thermal Spray Technology, 16, 1, pp. 40-63, 2007

Web page / page Web
http://dx.doi.org/10.1007/s11666-006-9010-7
http://nparc.cisti-icist.nrc-cnrc.gc.ca/npsi/ctrl?action=rtdoc&an=11708249&lang=en
http://nparc.cisti-icist.nrc-cnrc.gc.ca/npsi/ctrl?action=rtdoc&an=11708249&lang=fr

Thermal Spray Coatings Engineered from Nanostructured Ceramic Agglomerated Powders for Structural, Thermal Barrier and Biomedical Applications

(INVITED PAPER)

R. S. Lima* and B. R. Marple
National Research Council of Canada
75 de Mortagne Blvd.
Boucherville, QC J4B 6Y4
Canada

*** corresponding author**

Dr. Rogerio Lima
National Research Council of Canada
75 de Mortagne Blvd.
Boucherville, QC J4B 6Y4
Canada

Phone: +1-450-641-5150
Fax: +1-450-641-5105
e-mail: rogerio.lima@cnrc-nrc.gc.ca

Abstract

Thermal spray coatings produced from nanostructured ceramic agglomerated powders were tailored for different applications, some of which required almost completely opposite performance characteristics (e.g., anti-wear and abradable coatings). The influence of nanostructured materials on important areas, such as, thermal barrier coatings (TBCs) and biomedical coatings was also investigated. It was determined that by controlling the distribution and character of the semi-molten nanostructured agglomerated particles (i.e., nanozones) embedded in the coating microstructure, it was possible to engineer coatings that exhibited high toughness for anti-wear applications or highly friable for use as abradables, exhibiting abradability levels equivalent to those of metallic-based abradables. It is shown that nanozones, in addition to being very important for the mechanical behavior, may also play a key hole in enhancing and controling the bioactivity levels of biomedical coatings via biomimetism. This research demonstrates that these nanostructured coatings can be engineered to exhibit different properties and microstructures by spraying nanostructured ceramic agglomerated powders via air plasma spray (APS) or high velocity oxy-fuel (HVOF). Finally, in order to present readers with a broader view of the current achievements and future prospects in this area of research, a general overview is presented based on the main papers published on this subject in the scientific literature.

Keywords: nanostructured coatings, ceramics, microstructural characteristics, mechanical performance, biocompatibility.

1. Introduction

1.1 Nanostructured Materials

Nanostructured materials offer the potential for significant improvements in engineering properties based on improvements in physical and mechanical properties resulting from reducing the grain sizes by factors of 100 to 1000 times compared to present engineering materials, i.e., nanostructured materials exhibit grain sizes that are less than 100 nm in at least one dimension [1]. The Hall-Petch empirical relationship points to the potential of improving the mechanical properties of materials when decreasing the grain size [2]. In terms of yield strength and hardness, the expressions are:

$$\sigma_y = \sigma_0 + kd^{-1/2} \qquad (1)$$

$$H = H_0 + k'd^{-1/2} \qquad (2)$$

where σ_y and H refer to the yield strength and hardness of the material, respectively, the subscript *0* relating to the material's infinite grain size; k and k' are constants representing the grain boundary as an obstacle to the propagation of deformation (metal) or crack (ceramics); and d is grain size.

Equations 1-2 show that when reducing grain sizes from conventional levels (i.e., <10 μm in metals and <1-2 μm in ceramics) to nanostructured levels (i.e., <100 nm) the mechanical strength of materials can be considerably enhanced.

Another important class of nanostructured materials are carbon nanotubes. They were discovered in 1991 by Iijima [3]. They exhibit extraordinary mechanical, electrical and thermal properties. Carbon nanotubes exhibit the highest tensile strength known, approximately 200 GPa, i.e., 100 times stronger than the strongest steel with only 1/6 of its density. These are among the main reasons why, according to Koch [1], one of the most visible and growing research areas of nanoscience and technology is found in materials science.

1.2 Thermal Spray Coatings Engineered from Nanostructured Agglomerated Ceramic Powders

1.2.1 Nanostructured Ceramic Agglomerated Powders for Thermal Spray

In addition to bulk samples, the study of nanostructured materials has been extended to coatings processed using the thermal spray technique. The possibility of making coatings with superior wear resistance and more durable thermal barrier coatings (TBCs) when compared to the conventional thermal spray coatings currently available opens a wide range of research opportunities for ceramic materials. Thermal spray ceramic coatings are usually made from a powder feedstock. These powder particles typically exhibit a particle size distribution varying from 5 to 100 μm, i.e., the particles are microscopic. Fine particles, including nanosized particles, i.e., smaller than 100 nm, cannot be thermal sprayed using the regular powder feeders currently being employed in thermal spray. These tiny nanoparticles would clog the hoses and fittings that transport the powder particles from the powder feeder to the thermal spray torch.

In order to spray nanoparticles using regular powder feeders the nanosized particles are agglomerated via spray-drying (and then sintered) into microscopic particles. This process is usually employed when very fine materials such as nanostructured ceramic or cermet powders are to be thermally sprayed. Figure 1 shows a scanning electron microscope (SEM) image of the morphology of nanostructured titania (TiO_2) agglomerated powders for thermal spray [4]. It exhibits the typical donut shape of spray-dried particles (Fig. 1a). When the surface of this particle is analyzed at higher magnifications it is possible to observe the nanostructure of the feedstock (Fig. 1b), i.e., each microscopic titania particle is formed via the agglomeration of individual titania particles smaller than 100 nm.

Nanostructured ceramic agglomerated powders for thermal spray became available by the end of the 1990s. The information available to the authors indicated that the first materials available for research produced by nanotech industries (as opposed to in-house laboratory scale production) were nanostructured alumina-13wt% titania (Al_2O_3-13wt% TiO_2), nanostructured yttria stabilized zirconia (YSZ) (ZrO_2-7wt% Y_2O_3)

and nanostructured titania (TiO_2). Refereed papers on the microstructural characteristics and mechanical properties of the coatings produced from these powders began to be published in international materials science journals (*in English*) in 2000, 2001 and 2005 [4-10].

It is important to point out that to date there are not many nanotech companies producing agglomerated ceramic powders for thermal spray as a regular product line. Inframat Corp. (Farmington, CT, USA) [11] and Altair Nanomaterials Inc. (Reno, NV, USA) [12] can be cited as examples, as well as a new company, Millidyne Surface Technology (Tampere, Finland) [13], that has joined this nanotech thermal spray field. Current commercially available nanostructured agglomerated ceramic powders for thermal spray include Al_2O_3-13wt% TiO_2, ZrO_2-7wt% Y_2O_3, TiO_2, ZrO_2-8mol% Y_2O_3-NiO and ZrO_2-10mol% Y_2O_3. These nanotech companies may also produce customized nanostructured powders for specific applications on request.

Some researchers have chosen another route for the research and development of these coatings, i.e., the in-house production (at a laboratory scale) of nanostructured ceramic agglomerated powders. As previously stated, individual nanostructured particles are agglomerated via spray-drying (and then sintered) into microscopic particles. Spray-drying is a widely employed process and many research facilities have spray-driers at their disposal. Individual (i.e., non-agglomerated) nanostructured particles can be purchased and then agglomerated for research purposes at the laboratory scale. Among the first types of nanostructured ceramic agglomerated powders for thermal spray produced via this route were nanostructured alumina (Al_2O_3), nanostructured zirconia (ZrO_2) and nanostructured yttria stabilized zirconia (YSZ) (ZrO_2-7-8wt% Y_2O_3). Other researchers have produced the feedstock at a laboratory scale starting at the initial stage of manufacturing. Nanosized particles were produced via the chemical reaction method and subsequently agglomerated via spray-drying [14-16]. Refereed papers on the microstructural characteristics and mechanical properties of the coatings produced from these powders began to be published in international materials science journals (*in English*) in 2002 [14-19].

Currently many researchers are employing this method of agglomeration via spray-drying and sintering at the laboratory scale to produce nanostructured ceramic

powders for thermal spraying [20-29]. Other methods currently employed at the laboratory scale to prepare composite agglomerated ceramic powders are based on the mixing of two types of nanosized particles (e.g., Al_2O_3 and TiO_2 or ZrO_2 and Al_2O_3), usually via ball milling, spray-drying and sintering [30-34]. Finally, it is important to point out that in addition to the production of ceramic oxide powders via spray-drying and sintering, which are usually employed in anti-wear applications and as TBCs, nanostructured agglomerated hydroxyapatite (HA) ($Ca_{10}(PO_4)_6(OH)_2$) powders for biomedical applications are also being manufactured by the same method for subsequent thermal spraying [15].

1.2.2 Thermal Spraying Nanostructured Agglomerated Ceramic Powders

The thermal spray process is intrinsically associated with the melting of particles. Without some particle melting it is extremely difficult to produce thermal spray coatings, particularly with ceramic materials. Some degree of melting is necessary to achieve a sufficient level of particle adhesion and cohesion. This is a challenge for thermal spraying nanostructured powders; if all powder particles are fully molten in the thermal spray jet, all the nanostructural character of the powder particles will disappear, and therefore the thermal spray coating will not exhibit any nanostructured related property.

In order to overcome this challenge it is necessary to carefully control the temperature of the particles in the thermal spray jet, i.e., the temperature of the powder particles should be maintained such that it is not significantly higher than the melting point of the material. The particles must be thermally sprayed in such a way as to guarantee that part of the initial nanostructure of the feedstock will be embedded in the coating microstructure. Therefore these nanostructured feedstock powders tend to be quite sensitive to the spray parameters. The step for developing the spray parameters to achieve optimal coating performance can be time consuming. This optimization process is often facilitated by the use of diagnostic tools for monitoring the in-flight particle characteristics.

1.2.3 Bimodal Microstructure of Thermal Spray Coatings Engineered from Nanostructured Agglomerated Ceramic Powders

As previously stated, during the thermal spraying of these nanostructured agglomerated feedstock particles it is necessary to avoid full melting of the material in order to preserve part of the nanostructure and have it embedded in the coating microstructure. The coating microstructure is formed by semi-molten feedstock particles that are spread throughout the coating microstructure and are surrounded by fully molten particles that act as a binder, thereby maintaining coating integrity. As these coatings are formed by a mixture of particles that were fully molten and semi-molten in the spray jet, some authors have described these coatings as exhibiting a "bimodal microstructure" [30, 35-39]. A schematic of this bimodal microstructure is shown in Fig. 2.

An actual example of the bimodal microstructure can be found by looking at Figs. 3 and 4. Figure 3a shows a nanostructured agglomerated YSZ particle (Nanox S4007, Inframat Corp., Farmington, CT, USA). By looking at the particle at high magnification (Fig. 3b), it is possible to observe that the particle is formed via the agglomeration of individual YSZ particles with diameters varying from 30 to 130 nm. This powder was thermally sprayed using an air plasma spray (APS) torch (F4-MB, Sulzer Metco, Westbury, NY, USA). The temperature and velocity of the sprayed particles were monitored using a diagnostic tool (DPV 2000, Tecnar Automation, Saint Bruno, QC, Canada). This diagnostic tool is based on optical pyrometry and time-of-flight measurements to measure the distribution of particle temperature and velocity in the thermal spray jet. The average surface temperature and velocity of the thermally sprayed particles were 2563 ± 174°C and 208 ± 50 m/s, respectively [40]. This temperature is below the melting point of ZrO_2-7wt% Y_2O_3, reported to be approximately 2700°C [41]. Therefore it is expected that the spray jet impinging the substrate could be comprised of fully molten, semi-molten and even non-molten particles, i.e., part of the nanostructure of the nano YSZ powder was preserved and embedded in the coating microstructure, as shown in Fig. 4.

Figure 4 shows the microstructure of the coating produced by using the nanostructured agglomerated YSZ feedstock particles presented in Fig. 3. It is possible to

distinguish lighter-colored and darker-colored zones in the coating microstructure (Fig. 4a), i.e., the bimodal distribution. When looking at one of the darker-colored zones at higher SEM magnifications (Fig. 4b-c) it is possible to recognize the similarities between this type of zone and the morphology of the nano YSZ feedstock (Fig. 3b). The zones like those shown in Figs. 4b-c correspond to semi-molten nanostructured agglomerated YSZ particles that became embedded in the coating microstructure. Zones like those represented in Figs. 4b-c are also called "nanozones". The lighter-colored zones observed in Figure 4a probably represent particles that were fully molten in the plasma jet.

It is important to point out that by controlling the size, shape, and morphology of the bimodal distribution is it possible to engineer coatings with very pronounced differences in microstructural characteristics and mechanical performance. A key parameter is the density of the nanozones, as will be explained in Sections 2 and 3. Based on Figs. 1 and 3 it is clear that the nanostructured agglomerated particles comprising the feedstock are porous. Depending on thermal processing, spraying conditions and feedstock characteristics (e.g., diameter), the nanozones that form the coating may continue to be porous like the original feedstock (like those of Figs. 4b-c) or be much denser. The porous nanozones as expected to occur when the molten part of the agglomerated semi-molten particle does not fully infiltrate into its non-molten core during thermal spraying. On the other hand, the dense nanozones, as shown in the next section, probably occur when the molten part of an agglomerated semi-molten particle fully infiltrates into the small capillaries of its non-molten core, either in the spray jet or at impact with the substrate.

Finally it should be mentioned that most researchers and engineers involved in this new field of work employ the expression "nanostructured thermal spray coatings" to designate the thermal spray coatings produced from nanostructured agglomerated powders. As previously explained, for ceramic materials it is necessary to melt at least some fraction of the original nanostructure of the feedstock in order to achieve acceptable levels of coating adhesion and cohesion. Therefore part of the original nanostructure of the feedstock is destroyed during the regular thermal spray processing of ceramic materials. Consequently the expression "nanostructured thermal spray coating" is not strictly scientifically accurate for these cases. The expression "bimodal coating",

indicating the presence of particles in the coating microstructure that were semi-molten and fully molten in the spray jet, is more scientifically rigorous. However, the term "nanostructured thermal spray coatings" is widely used to differentiate this type of coating from those produced from conventional feedstock powders, which are generally called "conventional thermal spray coatings". Therefore, these two expressions will continue to be employed in this article.

2. Engineering Anti-Wear Thermal Spray Coatings by Using Nanostructured Ceramic Agglomerated Powders

2.1 Hardness and Toughness

It is important to point out that "conventional wisdom" seems not to work properly with these nanostructured thermal spray coatings concerning wear performance. For example, for ceramic oxide thermal spray coatings is generally considered that the harder coatings have the best anti-wear performance. Researchers working on APS nanostructured Al_2O_3-13wt% TiO_2 coatings observed that the nanostructured coatings exhibited wear resistance levels significantly higher than those of conventional ones (clad powder), however, the nanostructured coatings exhibited Vickers hardness values lower than those of conventional coatings [5-7, 33, 35-38]. Researchers working with other types of ceramic oxide compositions observed that the hardness levels of the nanostructured and conventional coatings were similar (when sprayed with the same type of torch). For example, this was found for Al_2O_3-3wt% TiO_2 (conventional fused and crushed powder) [31], YSZ (conventional hollow spherical powder "HOSP") [42] and TiO_2 (conventional fused and crushed powder) [10, 43, 44]; but it was also observed that the nanostructured coatings exhibited superior wear performance. However, other authors working on YSZ observed that the nanostructured coatings were harder and more wear resistant than the conventional ones (sintered and crushed and HOSP powders) [17, 21, 24, 25]. Turunen et al. [16] also observed that nanostructured Al_2O_3 coatings were harder and more wear resistant than the conventional ones (fused and crushed powder). It is important to point out that some authors did not observe superior wear behavior of the

nanostructured ceramic coatings, such as Al_2O_3-13wt% TiO_2 [45], when compared to the conventional material (clad and sintered and crushed powders). As previously stated in Section 1.2.2, the agglomerated nanostructured particles must be thermally sprayed by using controlled parameters to guarantee that part of the initial nanostructure of the feedstock will be embedded in the coating microstructure. Therefore if almost all nanostructured particles were fully melted in the spray jet, the coating will not exhibit any significant nanostructural character and the coating will tend to behave as a conventional material.

Several researchers cited in the previous paragraph have also observed that nanostructured thermal spray coatings exhibit significantly higher crack propagation resistance or relative toughness when compared to conventional coatings [6, 7, 10, 30, 35, 37, 38, 42, 44]. The crack propagation resistance (relative toughness) was evaluated and compared using Vickers indentation. At sufficient loads, during Vickers indentation, cracks form and propagate from or near the corners of the Vickers indentation impression. The shorter the crack propagation length, the higher the crack propagation resistance of the coating. Therefore, the higher wear resistance of the nanostructured ceramic thermal spray coatings is generally attributed to their higher crack propagation resistance, even if their hardness values are lower than or similar to those of the conventional ceramic thermal spray coatings [7, 10, 30, 35, 37, 38, 42, 44].

2.2 Origin of the Superior Toughness – Crack Arresting by Nanozones

The question that is now being raised is the origin of this superior toughness of nanostructured coatings. Does the nanostructure of the feedstock make a difference? Various authors have hypothesized and showed some experimental evidence to indicate that the semi-molten nanostructured particles embedded in the coating microstructure during thermal spraying tend to act as crack arresters, thereby increasing coating toughness [10, 35, 38, 44]. In order to understand this process it is necessary to look carefully at Figs. 5-8 [10].

Figures 5 and 6 show SEM pictures of the cross-sections of HVOF-sprayed titania coatings made from conventional (fused and crushed) and nanostructured (Fig. 1)

feedstock powders, respectively. Both coatings are very dense (porosity <1%) and do not exhibit the typical layered and lamellar microstructures of thermal spray coatings. In fact, it may be stated that these two coatings exhibit isotropic "bulk-like" microstructures. When the nanostructured coating is observed at high magnifications (Fig. 6b), it is possible to observe nanostructured regions that resemble the feedstock particle of Fig. 1. These types of regions correspond to semi-molten nanostructured titania feedstock particles that were embedded in the coating microstructure. As previously described, these nanozones are spread throughout the coating microstructure.

It is important to point out that the nanozones, such as that of Fig. 6b (which are dense) are very different from those of Figs. 4b-c (which are porous). As previously stated, the dense nanozones (Fig. 6b) probably occur when the molten part of a semi-molten particle fully infiltrates into the small capillaries of its non-molten core during thermal spraying. One important characteristic of these dense titania nanozones is the fact that the molten and non-molten phases do not show a significant difference in the contrast when observed via SEM. Therefore, due to the high densities of the nanozones and the overall coating, plus the lack of contrast difference between molten and non-molten TiO_2 phases, it is not easy to distinguish the semi-molten phases by using SEM at low magnifications, as was possible for the nano YSZ coating (Fig. 4). This is the reason why high SEM magnifications should be used for this coating to observe the semi-molten particles (Fig. 6b). By using X-ray diffraction it is possible to estimate the presence of semi-molten particles embedded in the coating microstructure. The nanostructured titania powder employed to make this coating is highly crystalline and exhibits anatase as the major phase and rutile as a very minor phase [46]. Its HVOF-sprayed coating is highly crystalline having rutile as the major phase and anatase as secondary phase [10]. By using the equation developed by Berger-Keller et al. [47], it was possible to determine the concentration of anatase (which was 25%) in the coating by comparing the intensities of the XRD peaks [101] of anatase and [110] of rutile. As the majority of the anatase phase transforms into rutile when melted and resolidified during thermal spraying [47], it is estimated that the percentage of dense nanozones embedded in the coating microstructure is approximately 25%. As previously stated, it is hypothesized that these nanozones have a fundamental role during crack arresting [10, 35, 38, 44], as shown in the results of crack

propagation resistance for conventional and nanostructured HVOF-sprayed titania coatings (Figs. 7-8).

The crack propagation resistance was determined by indenting the coating cross-sections with a Vickers indenter at a 5 kg load for 15 seconds, with the indenter aligned such that one of its diagonals would be parallel to the substrate surface. The total length (tip-to-tip) of the major crack (*2c*) parallel to the substrate surface that originated at or near the corners of the Vickers indentation impression was measured. Based on the indentation load (*P*) and *2c*, the crack propagation resistance was calculated according to the relation between load and crack length $P/c^{3/2}$ [48], where *P* is in Newtons and *c* is in meters. The crack propagation resistance values of the nanostructured and conventional coatings were 28.4 ± 1.4 MPam ½ and 17.2 ± 3.3 MPam ½, respectively [10].

When the conventional coating (Fig. 7) is compared to the nanostructured coating (Fig. 8), it is observed that the horizontal cracks of the conventional coating are more pronounced and longer than those of the nanostructured coating. The nanostructured coating exhibits shorter crack propagation under the same indentation load, therefore it is tougher. The Vickers hardness numbers (300 g) of the nanostructured and conventional coatings are 810 ± 26 and 833 ± 30, respectively [10]. The two coatings also show similar phase composition via X-ray diffraction (XRD), i.e., the same number of peaks (with similar intensities) corresponding to the same *hkl* indices appear on both coatings [10]. Therefore, as both titania coatings exhibit similar hardness values, phases and are near pore-free (<1%), it is thought that this comparison of crack propagation behavior is fair and meaningful, and the higher toughness of the nanostructured coating is a nanostructure-related effect. It is important to point out that the nanostructured thermal spray coatings are tougher than the conventional ones without having to compromise significantly the cohesive strength, i.e., hardness. As previously stated, "conventional wisdom" seems not to work properly with these nanostructured thermal spray coatings concerning wear performance.

The challenge is to experimentally demonstrate some evidence of the effect of the nanostructure on toughness. Some indication of this was found by observing the Vickers indentation crack tip at high magnifications. It was noticed that the crack had arrested after passing through a dense nanozone (Fig. 8b), i.e., a semi-molten nanostructured

particle where the molten part infiltrated into the small capillaries of the non-molten core during thermal spraying. Other authors have also experimentally observed the same behavior for APS nanostructured Al_2O_3-13wt% TiO_2 coatings [35, 38]. In conventional thermal spray ceramic coatings, a crack will tend to propagate through the coating's weakest link, which is the well-defined layered structure, i.e., the splat boundaries [49]. As previously described, in nanostructured coatings the splat structure is periodically disrupted by the nanozones. Therefore it is hypothesized that cracks propagating and reaching these well-embedded dense nanozones (Figs. 6b and 8b) tend to be arrested by them [10, 35, 38, 44]. On the other hand, by engineering the nanozones differently, such as making them porous (as those of Figs. 4b-c), it will create an opposite effect, i.e., the coating will become a friable ceramic abradable, as will be shown in Section 3.

To date there is no consensus on what percentage of the original nanostructural character of the feedstock (dense nanozones) that should be retained in the coating microstructure in order to produce an improved anti-wear coating. It is clear that by varying the quantity of semi-molten nanostructured particles (nanozones) embedded in the coating, very different mechanical behaviors are observed [7, 36-38]. For APS nanostructured Al_2O_3-13wt% TiO_2 coatings, it was found that the percentages of semi-molten particles embedded in the microstructure, which produced the best anti-wear coatings, were 15%-20% [7, 35, 37, 38] and 11% [33]. For APS nanostructured Al_2O_3-8wt% TiO_2, the best wear resistant coating exhibited a percentage of 25% of semi-molten particles embedded in the coating microstructure [34]. For the HVOF-sprayed nanostructured TiO_2 coating (Fig. 8), which exhibited a higher wear resistance when compared with the conventional one (Fig. 7), it was estimated via XRD that the percentage of semi-molten particles embedded in the coating microstructure was approximately 25%, as previously stated. It is important to point out that if the level of nanozones embedded in the coating microstructure is above or below an optimal value, the effects on mechanical properties will not be optimized [7, 35, 37, 38].

Finally, the crack propagation behavior under Vickers indentation of the conventional coating of Fig. 7 follows the typical character of thermal spray coatings, i.e., two cracks propagate parallel to the substrate surface from or near the corners of the Vickers indentation impression [50]. As previously stated, the cracks tend to propagate

parallel to the coating surface due to the weakest link offered by the layered structure of thermal spray coatings [49]. In other words, the crack tends to propagate along splat boundaries due to the weak intersplat bonding. Surprisingly, for the nanostructured coating (Fig. 8a), four cracks with similar lengths are observed originating at the four corners of the Vickers indentation impression instead of just two parallel to the substrate surface, i.e., the cross-section of the nanostructured coating is mechanically behaving like an isotropic material. The high density, high homogeneity, and isotropic bulk-like microstructure of the nanostructured coating (characteristics not typical of thermal spray coatings), probably have contributed to the propagation of four cracks, similar to what would be found when Vickers indenting an isotropic bulk ceramic material [48]. The conventional titania coating also exhibited high density, high homogeneity and isotopic bulk-like microstructure, however, no isotropic crack propagation was observed during Vickers indentation. This difference in behavior of these two coatings may lie in the nanostructural character of the feedstock. Further research is necessary in order to better understand this phenomenon.

2.3 Origin of the Superior Toughness – High Homogeneity of the Nanomaterial

It is also important to point out that a recent reference suggests a mechanism other than the nanozones and crack arresting effects for the improvement of the wear behavior of the APS nano Al_2O_3-13wt% TiO_2 coatings [33]. According to this reference [33], in the agglomerated nanostructured feedstock, the alumina and titania nanoparticles are intimately mixed. However, the same high homogeneity is not found in the conventional feedstock (clad particles), where fused and crushed microscopic alumina particles are covered by a thin layer of submicron titania particles. The addition of 13wt% of titania to alumina lowers the melting point of the compound, therefore due to the more intimate mixing of alumina and titania in the nanostructured powder, it was hypothesized that the molten and semi-molten nanostructured particles would arrive at the substrate surface and previously deposited layers with lower viscosity levels (higher degree of melting throughout the entire particle) than those of the conventional material. Consequently the splat-to-splat cohesion would be better for the nanostructured coating. In addition, it was

observed that the conventional coatings exhibited TiO_2-rich regions along the splat boundaries (a feature probably originating from the morphology of the feedstock), a characteristic not observed for the splat boundaries of the nanostructured coating. Again, this phenomenon was associated with the high homogeneity of the nanostructured feedstock. As titania has lower mechanical strength than alumina, the TiO_2-rich regions located along the splat boundaries of the conventional alumina-titania coatings could lead to poorer performance of this material. Therefore, according to Ahn et al. [33], the better wear resistance of the nanostructured coatings in their study was associated with the enhanced splat-to-splat strength of these types of materials, and not to crack arresting promoted by nanozones. Although this hypothesis has merit, it could be suggested that the nanostructured coatings should have higher values of hardness due to the enhanced intersplat contact. However, the data provided by Ahn et al. [33], indicated that the most wear-resistant nanostructured coating was softer than the conventional coating. In addition, this hypothesis does not explain the better wear behavior of nano TiO_2 coatings [10, 43, 44] and nano Al_2O_3 coatings [16].

Although further work is required to identify the mechanisms giving rise to the improved performance, it is a fact that when comparing nanostructured and conventional coatings produced from feedstock powders sprayed with the same type of torch, there can be a significant reduction in wear levels when employing nanostructured coatings. The literature indicates that these reductions varied from 21% to 75% for nano YSZ [17, 21, 24, 42, 51], was 32% for nano Al_2O_3 [16], was 39% for nano Al_2O_3-3wt% TiO_2 [31], varied from 71% to 75% for nano Al_2O_3-13wt% TiO_2 [7, 33, 35] and varied from 25% to 52% for nano TiO_2 [10, 43]. A summary of these results can be found in Table 1.

2.4 Enhanced Bond Strength of Nanostructured Ceramic Coatings

Some authors have observed enhanced bond strength of nanostructured thermal spray coatings employed in anti-wear applications. By using the ASTM standard C633 [52], it was observed that when comparing nanostructured and conventional coatings produced from feedstock powders sprayed with the same type of torch, the increase in bond strength for the nanostructured coatings was approximately 1.8 times higher for

APS nano Al_2O_3-13wt% TiO_2 [7] and 2.4 times higher for HVOF-sprayed nano TiO_2 [10]. The interfacial toughness values of APS nano and conventional (clad powder) Al_2O_3-13wt% TiO_2 coatings were measured and compared via the Rockwell indentation method. It was found that this value was 2 times higher for the nanostructured coating [39].

The higher bond strength of the nanostructured coatings was explained by this higher interfacial toughness observed by Bansal et al. [39]. For the conventional coating it was observed that the interfaces between the particles that were fully molten in the spray jet and the steel substrate exhibited microcracks. For the nanostructured coating it was observed that the interfaces between the particles that were semi-molten in the thermal spray jet (i.e., dense nanozones) and the steel substrate were adherent, i.e., no microcracks or gaps. Therefore an interfacial crack in the nanostructured coating would tend to be interrupted by the strong adherent dense nanozones, thereby increasing interfacial toughness and bond strength. This phenomenon is somewhat similar to that hypothesized for the better wear performance for the nanostructured coatings, which also involves the presence of dense nanozones.

2.5 Plasticity of Nanostructured Ceramic Coatings

Various researchers have observed after wear tests that the wear scar of nanostructured coatings is smoother than that of the conventional ones. This higher plasticity of the nanostructured coatings is a phenomenon observed for nano Al_2O_3-13wt% TiO_2 [35], APS nano YSZ [17] and HVOF-sprayed nano TiO_2 [10], when compared to conventional coatings sprayed from clad, sintered and crushed, and fused and crushed powders, respectively. The more smeared appearance of the wear scars of the nanostructured coatings seemed to indicate that plastic deformation was the main wear mechanism that occurred during wear, whereas, cracks, delamination and microfracture observed on the wear scars of the conventional coatings indicated that brittle fracture was the main wear mechanism. The differences in morphology of the wear scars of nanostructured and conventional coatings described above can be observed by looking at Figs. 9 and 10.

There is a hypothesis to explain this behavior. It has been shown that plastic deformation (i.e., ductile flow) and fragmentation (i.e., brittle fracture) occur during grinding of thermal spray coatings [53, 54]. During the grinding of a ceramic material, a transition of material removal mechanism from ductile mode to brittle mode occurs. The initial ductile flow progressively changes to brittle fracture after a critical depth of cut is reached. The critical depth of cut of a ceramic material is directly proportional to its toughness-to-hardness ratio [53, 54]. Therefore, nanostructured and conventional ceramics tend to exhibit similar values of hardness, but as nanostructured coatings have higher values of toughness, it can be hypothesized that the nanostructured coatings should also exhibit a higher critical depth of cut. This higher critical depth of cut (i.e., large region of plastic deformation) should translate into a smoother wear scar, as observed by various researchers [10, 17, 35].

This enhanced plasticity of the nanostructured coatings may be beneficial during the process of grinding and polishing of thermal spray coatings. Grinding and polishing thermal spray coatings is generally required, mainly for anti-wear applications. This process can be very expensive and time consuming. Therefore having a coating that is easier to polish constitutes a very important advantage.

2.6 HVOF Spraying of Nanostructured Ceramic Coatings – A New Approach for High Performance Anti-Wear Coatings

Recently, various researchers have published papers on the mechanical properties of HVOF-sprayed ceramics [10, 16, 44, 45, 55-58]. It was observed that HVOF-sprayed conventional TiO_2 coatings exhibited very high Weibull modulus values of hardness when compared to those of other thermal spray coatings in the literature [55, 56]. This characteristic means that the distribution of hardness values of the coating was very narrow, i.e., it was a mechanical indication of the high homogeneity of the coating microstructure. This is highly desirable in a ceramic material because the probability of failure under mechanical stresses would be diminished. This high Weibull modulus value was attributed to the very dense and homogeneous ceramic coating microstructure

produced by employing HVOF, features which have also been observed by other researchers [16, 57, 58].

Due to this high uniformity of HVOF-sprayed conventional ceramic coatings, the use of nanostructured powders has been studied to determine if further improvements in the wear performance could be obtained over that produced by the air plasma spraying of nanostructured ceramics. Conventional (fused and crushed) and nanostructured TiO_2 powders were sprayed by APS and HVOF. From the APS conventional to the HVOF-sprayed conventional TiO_2 coatings there was a reduction in the wear levels of 44%. However, from the APS conventional to the HVOF-sprayed nanostructured TiO_2 coatings there was a reduction in the wear levels of ~60% [44]. In addition, the bond strength (ASTM C633 [52]) of the HVOF-sprayed nano TiO_2 coating was 1.6 times higher than that of the APS conventional one. Fatigue studies demonstrated that the average fatigue life of HVOF-sprayed nano TiO_2 was 1.7 times higher than that of APS conventional TiO_2 [59].

The abrasion wear behavior of conventional (clad and blended powders) and nanostructured Al_2O_3-13wt% TiO_2 coatings sprayed by APS and HVOF was also compared [60]. From the APS conventional to the APS nanostructured Al_2O_3-13wt% TiO_2 coatings there was a reduction in the abrasion wear rate of 33%. From the APS conventional to the HVOF-sprayed conventional Al_2O_3-13wt% TiO_2 coatings there was a reduction in the abrasion wear rate of 50%. However, from the APS conventional to the HVOF-sprayed nanostructured TiO_2 coatings there was a reduction in the wear levels of ~90%. A summary of the wear results achieved from spraying conventional ceramics by APS (traditional method) to spraying nanostructured ceramics via HVOF (alternative method) can be found in Table 2.

HVOF-spraying of nanostructured ceramics may also produce unexpected results. For example, TiO_2 is in general a material considered to be of lower wear resistance when compared to Al_2O_3-13wt% TiO_2. However, when the abrasion behavior of an HVOF-sprayed nano TiO_2 coating (Figs. 6 and 8) was compared to that of APS conventional Al_2O_3-13wt% TiO_2, a reduction of 27% in the wear levels was observed by employing the nanostructured coating [4]. The APS conventional Al_2O_3-13wt% TiO_2 coating was 25% harder than the HVOF-sprayed TiO_2 coating, however, the crack

propagation resistance of the nanostructured coating was 1.9 times higher than that of the conventional one. Once again, the high toughness of the nanostructured coating proved to be a very positive characteristic.

Spraying ceramic materials by HVOF is a challenge due to the high melting point of ceramic materials and the low flame temperatures of HVOF torches, which are generally below 3000°C. In addition, fine feedstock powders, typically from 5 to 25 microns, have to be employed for producing high quality ceramic coatings at acceptable deposition efficiency levels [55, 56]. Nonetheless, the wear performance of HVOF-sprayed nanostructured ceramics seems to be unmatched by that of APS conventional ceramics.

3. Engineering Abradable Coatings by Using Nanostructured Ceramic Agglomerated Powders

3.1 Abradable Seals

Thermal spray abradable seal coatings are a specially designed class of materials used to reduce gas path clearance in gas turbine engines. The clearance between the rotating blades and the casing should be as small as possible in order to increase the efficiency and reduce fuel consumption of aircraft and land-based turbines. Abradable coatings are characterized by a friable structure produced by a carefully selected material composition. These coatings are difficult to engineer because they must be at the same time readily abradable and mechanically stable to withstand the harsh operating conditions of a gas turbine. The abradable coating is normally a composite material composed of a metal phase, self-lubricating non-metal phase and many pores [61].

3.2 Abradables for High Temperatures

There is an increasing demand from the aerospace and energy industries for the production of turbines that operate at higher temperatures. Operation at higher temperatures is translated into higher efficiency, higher economy and less pollution. As a

consequence, the abradable coatings used in these applications must also follow this trend, i.e., they must be able to operate at higher temperatures. In order to achieve this goal, two main types of high temperature abradables are currently in use. The first one is based on the combination of a high temperature alloy (CoNiCrAlY), a self-lubricating material (boron nitride - BN) and a polymer (polyester) [40]. The metallic alloy provides the oxidation resistance and mechanical integrity at high temperatures. The BN lowers the friction coefficient of the coating and the polyester produces high amounts of porosity (producing a friable structure) after it is burned out of the coating microstructure. The second type of high temperature abradable currently in use is based on a ceramic material (ZrO_2-7wt% Y_2O_3), BN and polyester [62]. The ceramic material provides the mechanical and chemical integrity at high temperatures. Like the metallic abradable, the BN also lowers the friction coefficient and the polyester also creates a network of porosity in the coating microstructure (after being burned out), therefore making a ceramic material friable. Despite the success of the current approach, there are still problems to be solved. For example, when spraying a composite material having constituents with very different physical properties, such as CoNiCrAlY and polyester or ZrO_2-7wt% Y_2O_3 and polyester, it is very difficult to have consistency in the spraying process. Therefore these types of coatings tend to be rather inhomogeneous. In addition, before using the coating it is necessary to burn the polymer phase out of the coating microstructure. This process requires additional time and adds to the total cost. Therefore, as indicated by Ghasripoor et al. [63], a 100% ceramic coating for use as a high temperature abradable could represent a major advance in the development process and produce the next generation of abradable materials.

3.3 Engineering Nanostructured Ceramic Abradables

As previously demonstrated in Section 2, nanostructured ceramic thermal spray coatings exhibit enhanced wear resistance when compared to the conventional materials. It is important to point out that the requirements of an abradable coating are opposite to those of an anti-wear coating. Therefore based on these facts and the scientific findings,

summarized in earlier sections, the approach for engineering a ceramic abradable from a nanostructured feedstock is not obvious.

It was observed that a key feature to engineer friable nanoceramic coatings is to employ a very porous nanostructured agglomerated ceramic particle as feedstock, such as the nano YSZ particle of Fig. 3. It is likely the mechanical strength of this type of particle (e.g., if measured via nanoindentation), would be very low. Therefore, by embedding a significant amount of these semi-molten porous particles in the coating microstructure, the ceramic coating would probably become friable, possibly producing a nanostructured ceramic abradable coating. As previously stated in Section 1.2.3, depending on thermal processing, spraying conditions and feedstock characteristics (e.g., diameter), these nanozones may remain porous like the original feedstock. The porous nanozones occur when the molten part of the agglomerated semi-molten particle does not fully infiltrate into its non-molten core during spraying.

Figure 4 shows a nanostructured ZrO_2-7wt% Y_2O_3 coating engineered to be an abradable seal by air plasma spraying a nanostructured ZrO_2-7wt% Y_2O_3 feedstock like the one shown in Fig. 3 [40]. The abradability of this coating was tested in a rub-rig testing facility, which can simulate operating conditions of typical gas turbine engines. The abradability of this material was compared to that of an APS CoNiCrAlY-BN-polyester coating, which represents one of the state-of-the-art high temperature abradable seal materials currently available. In order to obtain preliminary results, all the tests were carried out at room temperature. The blade (width: 6 mm / thickness: 3 mm) material employed was Inconel 718.

Figures 11 and 12 show pictures of the wear scars of the nano YSZ and the CoNiCrAlY-based abradable coatings, respectively. The abradability test was carried out by setting a blade tip speed of 310 m/s, an incursion rate of 2.5 μm/s and a total incursion of 1 mm [40]. The average volume loss values of the nano YSZ and CoNiCrAlY-based abradable coatings after the rub-rig test were found to be 132 ± 8 mm^3 ($n = 2$) and 131 ± 2 mm^3 ($n = 2$), respectively. Therefore, both pure ceramic and metallic-based abradables exhibited the same volume loss under the same testing conditions. The wear of the blade tip was negligible for both cases. In addition, the wear scar of the nano ceramic coating shows a "clean-cut" structure and no chipping and/or macrocracking were observed.

Metallic residues from the metallic blade embedded in the wear scar were not visually identified. Consequently, this ceramic coating was very friable. The wear scar of the nanostructured coating was also smoother than that of the metallic-based abradable, which may indicate that the nanoceramic abradable could have better sealing properties. The percentage of semi-molten nanostructured porous particles embedded in the coating microstructure was 30-35%.

This work showed that a material that is generally considered as being hard and stiff can be engineered to produce a nanostructured 100% ceramic coating with a friable structure possessing attributes required for an abradable coating [40]. This work will continue by testing these coatings in a high temperature rub-rig testing facility. Finally, it is important to point out that if the molten part of the semi-molten nano YSZ particles fully infiltrated in their non-molten cores during thermal spraying, this coating would probably exhibit enhanced anti-wear performance.

A more rigorous scientific understanding of the "good" performance of the nano YSZ coating as an abradable can be found in a previous work [36]. It was demonstrated that by engineering ceramic thermal spray coatings with significantly different amounts and morphologies of porous semi-molten nanostructured particles (porous nanozones) embedded in the coating structure, very hard or very soft zones could be produced in the microstructure. Consequently, by engineering the spray parameters and powder morphology, it could be possible to produce ceramic coatings with a large concentration of low mechanical integrity or soft zones (porous nanozones), which would probably make a ceramic coating with a low cohesive strength.

4. Engineering Thermal Barrier Coatings by Using Nanostructured Ceramic Agglomerated Powders

4.1 Thermal Diffusivity and Thermal Expansion of Nanostructured TBCs

Chen et al. have measured the thermal diffusivity of APS nanostructured and conventional YSZ coatings up to 1200°C during heating and cooling stages [23]. The thermal diffusivities of the nanostructured and conventional YSZ coatings in the

measured temperature range were 1.80-2.54 X 10^{-3} cm^2/s and 2.25-3.57 X 10^{-3} cm^2/s, respectively. These thermal diffusivity values for the nano YSZ coating are lower than those reported in the literature for conventional YSZ coatings under the same temperature range [64, 65]. An explanation for this lower thermal diffusivity of nano TBCs is not clear. It may be related to the presence of a nanoporosity network within each single nanozone, as observed for the nano YSZ coating of Fig. 4. Thermal spray coatings exhibit globular and intersplat porosities. The porous ceramic nanozones spread throughout the coating microstructure, in addition to the regular globular and intersplat porosities of thermal spray coatings, may help to lower even further the overall thermal diffusivity of the coating.

The coefficient of thermal expansion (CTE) of the nano and conventional coatings were also measured for the same temperature range. From 300°C to 1200°C, the CTE of the nano YSZ coating was slightly higher than that of the conventional one [23].

4.2 Thermal Shock Resistance of Nanostructured TBCs

Liang and Ding evaluated the thermal shock resistance of nano and conventional (fused and crushed powder) YSZ coatings by heating them in a furnace for 30 min. at a series of temperatures up 1300°C, followed by subsequent cooling (dropping) in cool water for 10 min. [26]. For the thermal shock tests carried out at temperatures from 1000°C to 1300°C, the number of cycles to failure of the nano YSZ coatings was approximately 2-3 times higher than that of the conventional coatings.

It was observed that the thermal shock behavior of the nano YSZ coating was very different from that of the conventional YSZ coating. Vertical cracking propagating from the surface, which increased with an increase in the number of thermal cycles, were observed for the nano YSZ. It was reported that the cracks propagated slowly down to the bond coat without further horizontal propagation at the top coat/bond coat interface [26]. This horizontal crack propagation resistance may be attributed to the presence of nanozones at the interface, as described by Bansal et al. [39]. The conventional YSZ coating did not exhibit vertical cracks, instead, horizontal cracks were observed, especially near the top coat/bond coat interface [26].

Transmission electron microscope images of the thermally cycled coatings have shown that the nano YSZ coatings exhibit intergranular fracture, whereas, for the conventional coating, intergranular as well as transgranular fractures were observed [26]. Intergranular fracture is preferred for enhancing the thermal shock resistance due to the increased tortuosity of the fracture path.

Wang et al. also evaluated the thermal shock resistance of nano and conventional (fused and crushed powder) TBCs [28]. The coatings were heated to 1200°C for 5 min. in a furnace and quenched in water at room temperature. The number of cycles to failure of the nanostructured YSZ coating was 2-4 times higher than that of the conventional coating, i.e., a result similar to that of Liang and Ding [26]. A summary of the results of the thermal shock tests can be found in Table 3.

The higher thermal shock resistance of the nano TBCs may be caused by an enhanced toughness of this material. This high toughness may be associated with the presence of nanozones (as previously described), which are hypothesized to toughen the coating through crack arrest; however, no experimental evidence has been provided to support this hypothesis in TBCs. As postulated for the thermal diffusivity, the higher thermal shock resistance may be related to the presence of a nanoporosity network within each single nanozone, as observed for the nano YSZ coating of Fig. 4. Porous ceramic nanozones spread throughout the coating microstructure may enhance the compliance of the coating enabling it to perform better when subjected to a stress such as that caused by thermal shock, thereby increasing the number of cycles to failure of these coatings.

4.3 Sintering Effects on Nanostructured TBCs

One of the main concerns about the use of nanostructured thermal spray coatings at high temperatures (e.g., like a TBC) is their stability in relation to sintering-related effects. Sintering effects may harden and stiffen a nano TBC causing a premature failure. Various researchers have observed the effects of high temperatures on the nanostructured regions (nanozones) of nano TBCs [29, 66-68]. The agglomerates employed to make these coatings exhibited individual nanosized YSZ particles with diameters ranging from 15 nm to 130 nm. After 50 h at a temperature of 1100°C, the individual nanostructured

particles contained in the semi-molten agglomerates reached diameters of the order of 300 nm [29]. Wang et al. [66] reported a very low growth rate, where the nanoparticles reached 90 nm of diameter after 1150°C for 300 h. According to Racek et al. [67], the diameters of the nanostructured particles were larger than 400 nm when treated at 1300°C for 30 h. The nano YSZ coating of Fig. 4 was exposed at a temperature of 1000°C for 48 h [68]. It was observed that the individual nanostructured YSZ particles exhibited diameters of approximately 250 nm. In all these cases it was observed that the nanoporosity network exhibited in the nanozones such as that of Fig. 4, tended to be healed at high temperatures.

4.4 Creep Behavior of Nanostructured TBCs

The nano YSZ coating shown in Fig. 4 was submitted to creep testing at 1000°C for 48 h. As mentioned earlier, the percentage of semi-molten nanostructured zones embedded in the microstructure of this coating was approximately 30-35%. Its behavior was compared to that of a conventional TBC [68]. The creep strain rate for the nano YSZ coating was higher than that of the conventional (HOSP powder) YSZ, with activation energies of 165 and 192 kJ/mol and stress exponents of 2.2 and 1.3 for the nano and conventional YSZ coatings, respectively. The dominant creep mechanisms giving rise to the higher creep strain rate of the nano YSZ were identified as grain boundary sliding and the rearrangement of the nanoparticles (in the nanozones).

The higher creep rate of the nano YSZ would result in an enhanced relaxation during stress at elevated temperatures, which is a desirable phenomenon. However, this enhanced relaxation at high temperatures may lead to the development of stresses during cooling, which could cause premature failure of the coating. On the other hand, as previously shown, nanostructured coatings tend to exhibit higher toughness when compared to conventional ones, which may outweigh the stress effect during cooling [68]. In addition, as previously shown, thermal shock tests have demonstrated a superior thermal shock behavior of nano TBCs [26, 28].

5. Engineering Nanostructured Ceramic Coatings for Biomedical Applications

5.1 Biomedical Thermal Spray Coatings

Metallic implants, such as hip joints, are used to replace body parts that no longer function properly due to degradation from wear, disease or injury. Such implants are normally made of titanium alloys (Ti-6A1-4V). These alloys exhibit high mechanical strength and cause no harm to the human body. They are bioinert. However, due to their lack of biointeraction, they do not form strong bonds between the metal surface and the bone cells, known as osteoblasts. Another agent must be employed to assist in the attachment of the metallic implant to the osteoblast cells, also known as osseointegration.

One way to promote osseointegration and bonding between the implant and the surrounding bone is the use of a biocompatible coating, such as hydroxyapatite (HA) [15], that is well bonded to the surface of the implant (prosthetic device). This coating is normally applied by a thermal spray technique prior to implantation in the body. Following implantation the osteoblast cells attach to the biocompatible coating, thereby providing an increased rate of apposition and bonding.

5.2 Enhanced Biocompatibility of Nanostructured Materials

It has been demonstrated that nanostructured ceramic materials, such as, alumina (Al_2O_3), titania (TiO_2) and HA exhibit enhanced biocompatibility with osteoblast cells (i.e., bone cells) when compared to their conventional counterparts [69-72]. This enhanced biocompatibility is translated into higher cell reproduction and adhesion on the surface of these materials, which are very important characteristics for making implants with improved bioperformance and longevity. Webster et al. [71] explained this better performance of the nanostructured material as the effect of the nanotexture or nanoroughness of these materials on the adsorption of the adhesion proteins like vitronectin and fibronectin. These types of proteins mediate the adhesion of anchorage-dependent cells (such as osteoblasts) on substrates and coatings [71]. These adhesion

proteins are initially adsorbed on the surface of an implant almost immediately upon its implantation in the human body. When the osteoblast cells arrive at the implant surface they "see" a protein-covered surface that will connect with the transmembrane proteins (integrins) of the osteoblast cells. It is important to point out that these proteins, such as fibronectin, exhibit nanosized lengths and structures. For example, the average size of fibronection is about 150 nm [73]. It is interesting to note that the surface of a nanostructured material (nanosized grains) will exhibit nanocharacteristics, such as nanoroughness, whereas, the surface of a conventional material (microsized grains) will exhibit microcharacteristics. It has been proven that the interaction or the adsorption of a nanosized protein (e.g., vitronectin and fibronectin) to a nanotextured surface will be more effective than that provided by a microtextured one [71].

As shown schematically in Fig. 2, the nanozones of the bimodal coatings are spread throughout the coating microstructure, and are present even at the coating surface. Therefore the use of a nanostructured thermal spray coating, containing regions on its surface exhibiting nanotexture (nanoroughness), has been investigated as a method for improving the adhesion of osteoblast cells on the coating, with the goal of producing a better long-term performance of implants. An additional consideration is the good mechanical performance of the nanostructured coatings that also contributes to enhancing the longevity of the implant. Therefore, in the biomedical coatings to be discussed in the following sections, the nanozones have a dual function: improving the mechanical performance and enhancing the biocompatibility.

5.3 Nanostructured Hydroxyapatite Coatings

A nanostructured agglomerated HA powder particle is shown in Fig. 13. It was formed by spray-drying and sintering. The individual nanosized HA particles are elongated with lengths less than 500 nm and widths up to 100 nm [15]. Only HA peaks were detected by XRD. These particles were HVOF-sprayed at an average in-flight temperature of 1826± 82°C and average particle velocity of 638 ± 82 m/s. The high velocities of the sprayed particles at the point of impact resulted in a highly dense coating

(Fig. 14). It is possible to observe the low degree of porosity (porosity: 1.4 ± 0.1%) and the layered structured of the coating [15].

For this coating, only HA peaks were detected in the XRD spectrum, i.e., no secondary phases such as as tricalcium phosphate (TCP), tetracalcium phosphate (TTCP) or calcium oxide (CaO) were present. The presence of two humps in the XRD spectrum indicated that some amorphous calcium phosphate (ACP) was also present in the coating, however, the relative crystallinity of this coating was found to be 84%. It is interesting to analyze this low degradation of the HA during HVOF spraying. According to the phase diagram for the system $CaO\text{-}P_2O_5\text{-}H_2O$, the HA decomposes at ~1550°C to a mixture of $Ca_3(PO_4)_2$ (TCP), $Ca_4P_2O_9$ (TTCP) and water [74]. The melting point of the mixture of TCP and TTCP formed by the decomposition of HA is ~1570°C. Based on the average particle temperature (1826± 82°C), it is observed that many particles exhibit temperatures above 1550°C. However, as was previously stated, the degradation of the HA coating was very low and its crystallinity was very high. These are strong indications that the majority of HA particles did not fully melt or undergo phase transformations during HVOF spraying. It is important to point out that these temperatures are measured via pyrometry, i.e., they represent values of temperature at the particle surface. Therefore the temperatures inside the particles may exhibit lower or higher values. It is important also to note that based on the particle velocity measurement (638 ± 82 m/s) and spray distance (20 cm), the sprayed particles would take less than a millisecond to travel from the torch to the substrate. As a consequence, the time exposure at high temperatures is very limited [15].

Based on these results it is possible to infer that part of the original nanostructure of the feedstock was probably preserved during thermal spraying and was embedded in the coating structure. Figure 15 shows different types of nanozones present in the coating microstructure (cross-section) as observed using an SEM at high magnification. The nanozones shown in Fig. 15a is porous, like the porous structure of the HA particle (Fig. 13). It is thought that Fig. 15a represents an HA particle that was partially molten at impact with the substrate. The individual nanosized particles of the feedstock became rounded but they did not coalesce during spraying. Therefore the porous structure of the agglomerated feedstock was kept intact. Figure 15b exhibits a nanostructured fibrous

zone. It is possible to distinguish rounded particles embedded in the fibers, which indicate that probably this region was partially molten and there was some coalescence during flight or at impact. Figure 15c shows another type of nanostructure. It is possible to observe nanosized spherical particles densely packed, which were probably formed by the melting and coalescence of the elongated nanosized particles of the feedstock [15]. Recently Li and Khor [75] have also observed similar types of nanostructures by spraying nano HA using plasma-spray and HVOF.

Unfortunately, superior mechanical performance, such as bond strength (ASTM C633 [52]) was not achieved by employing nanostructured HA feedstock powders. The bond strength of the HVOF-sprayed nano HA coating of Fig. 14 on Ti-6Al-4V substrates was 24 ± 8 MPa. Li and Khor observed maximum bond strength of 31 MPa for an HVOF-sprayed nano HA coating [75]. These bond strengths are not higher than some of the highest bond strength values reported for APS (27 MPa) [76] and HVOF-sprayed (31 MPa) [77] conventional HA coatings sprayed on Ti-6Al-4V substrates. The ordinary bond strength values achieved by nano HA coatings were probably related to its inherent low mechanical strength, which was probably not affected by the presence of the nanostructure.

At least some effect of the nanostructured feedstock on the biocompatibility was observed. According to Li and Khor [75], by employing an osteoblast cell culture (*in vitro*) it was observed that the phase composition of the HA coatings had a more pronounced effect on attachment and proliferation of the osteoblast cells than the nanostructure, however, the HA coatings with a high content of both crystalline HA and nanostructures were preferred for cell proliferation.

5.4 Concerns Regarding the Long Term Performance of Hydroxyapatite Coatings

As mentioned in Section 5.1, HA coatings deposited by APS are routinely applied on metallic hip-joint implants to promote the fixation of the implant to the bone. This is one of the most common methods to promote this fixation. APS HA coatings are a success and they may be considered the state-of-the-art for the current thermal spray standards. Despite the success of APS HA coatings, there are still concerns regarding

their long-term performance, i.e., the stability of the HA in the human body. HA is a material that exhibits low values of mechanical strength and toughness. In addition, it is widely known that HA coatings exhibit dissolution and are affected by osteolysis (pathologic process involving resorption of bone surrounding the implant) in vivo [78]. This dissolution and/or osteolysis may lead to a weakening of the coating. In fact, reports in the medical literature show that the rate of aseptic loosening and/or osteolysis of HA-coated implants can be high, mainly for the acetabular cup. According to Reikeras and Gunderson [79], after 10 years post-operation, 20% of the HA-coated acetabular cups in patients in their study were revised due to aseptic loosening and/or osteolysis. Blacha [80] observed a failure rate of 23% of the HA-coated acetabular cups, caused by aseptic loosening and/or osteolysis, after an average of 6 years post-implantation. In a study by Lai et al. [81], 18% of the HA-coated acetabular cups exhibited aseptic loosening and/or osteolysis after an average of 10 years post-implantation. Lai et al. [81] demonstrated that there is a strong correlation between aseptic loosening and/or osteolysis and the residual amount of HA coating covering the implant. Other factors also contribute to the concerns over the long-term performance of HA coatings. The resorption/dissolution of HA is significantly accelerated during loading [82], which is not a desirable characteristic if a hip-joint is implanted in young and active patients. To address these issues, work has been performed to identify a non-absorbable coating, with excellent mechanical performance and nanostructural characteristics that could serve as an interesting alternative to replace APS HA coatings in implants for young and active patients.

5.5 Superior Mechanical Performance of Nanostructured TiO_2 Coatings

As previously stated, the HVOF-sprayed nanostructured TiO_2 shown in Figs. 6 and 8 has demonstrated superior mechanical performance when compared to its conventional counterparts [4, 10, 44, 59]. TiO_2 is also a material that does not dissolve in human body fluids. Moreover, it has been demonstrated that nano TiO_2 bulk ceramics exhibit higher biocompatibility levels when compared to those of conventional TiO_2 [69-72]. Therefore due to (i) the superior mechanical performance of the HVOF-sprayed titania coating made from the nanostructured feedstock, (ii) the non-toxic nature of TiO_2

and its stability in the human body, and (iii) the possibility of producing nanotextures on the surface of the coatings, these types of coatings have been investigated as candidates to replace APS HA coatings on implants, mainly for younger patients.

Measurement of the bond strength (ASTM C633 [52]) of the HVOF-sprayed TiO_2 coating on Ti-6Al-4V substrates [46] resulted in failure of the adhesive (at 77 MPa) used in the test. At this point the coating was still well adhered to the substrate, indicating that the bond strength value of the nanostructured TiO_2 coating was higher than 77 MPa. Consequently, the bond strength value of the nanostructured titania coating is at least 2.5 times that of the highest bond strength value found in the literature for an HA coating, which is around 31 MPa [77]. The hardness measurements show also an important improvement. The Vickers hardness of the HVOF-sprayed nanostructured titania coating is 61% higher than that of the bulk (sintered) HA [83] and more than 3 times that of a plasma sprayed conventional HA [84].

5.6 In Vitro and In Vivo Tests with Nanostructured TiO_2 Coatings

After the mechanical tests indicated that this type of coating exhibited excellent mechanical performance when compared to HA coatings, biocompatibility tests were also carried out and the preliminary results were encouraging. Ti-6Al-4V disks were coated with HVOF-sprayed nano TiO_2 (Figs. 6 and 8) and APS conventional (sintered and crushed powder) HA coatings. In vitro osteoblast (obtained from rat calvaria) cell culture was carried out for a period of up 15 days [85]. The same number of cells was seeded on both coatings. After 7 days of incubation, one sample of each coating was taken for SEM analysis. Figures 16 and 17 show the osteoblast cells on the surface of the HVOF-sprayed nano TiO_2 and APS conventional HA coatings after 7 days of incubation, respectively. It is observed that after 7 days the osteoblast cells almost completely covered the surface of the nano TiO_2 coating, whereas, the surface of the APS conventional HA coating was partially covered. Following this initial qualitative test, a quantitative test based on alkaline phosphatase activity (ALP) was carried out after 15-day incubation. The cell colonies were fixed and stained for alkaline phosphatase activity, which produced a red stain over the coatings [85]. In the ALP test, the percentage of the coating covered in red

is a measure of the osteoblast cells' ability to adhere, proliferate, and differentiate on the coating surface. The ALP red signal was quantified with image analysis and is shown in Fig. 18. It is possible to observe that the degree of cell proliferation on the nano TiO_2 coating (measured by the relative intensity of red staining) was at least equivalent to or maybe superior to that of the HA coating. This preliminary result agrees with the qualitative results shown in Figs. 16 and 17. These results, although preliminary, are somewhat unexpected because HA is often considered as the most efficient biocompatible material.

In vivo experiments were also carried out with these HVOF-sprayed nano TiO_2 coatings. These coatings were deposited on small Ti-6Al-4V rods that were subsequently implanted in the femur of rabbits. Grit-blasted Ti-6Al-4V rods without coating were also implanted and served as a control. A total of five nano TiO_2 coated and six uncoated Ti-6Al-4V were implanted. After 7 weeks of implantation the rabbits were euthanized and the contact surface between the bone and implant was measured via optical microscopy. On average, the contact surface between the HVOF-sprayed nano TiO_2 coating and bone was 1.7 times higher than that of the uncoated Ti-6Al-4V rods.

5.6 Relationship between Biocompatibility and Nanostructure in the TiO_2 Coatings

There is a hypothesis that may help explain this "good" biocompatibility of the HVOF-sprayed nano TiO_2 coating observed in these preliminary in vitro and in vivo results. As previously stated in Section 5.1 (based on other researchers' findings for bulk materials [69-72]), the use of a nanostructured thermal spray coating, containing regions on the surface exhibiting nanotexture (nanoroughness), appears to be an attractive method for improving the adhesion of osteoblast cells on the coating and contributing to a better long-term performance of the implant. When the surface of the nano TiO_2 coating of Figs. 6 and 8 is analyzed via high magnification SEM, it is possible to observe nanostructured zones (Fig. 19), which were formed from partially melted nano TiO_2 particles like that of Fig. 1 that were incorporated into the coating after becoming semi-molten in the spray jet. It is hypothesized that these nanozones could interact (e.g., serve as anchors) with nanosized adhesion proteins, such as fibronectin (150 nm) [73], which

could lead to the formation of a biomimetic structure [86]. This biomimetism may help to increase the adhesion strength of the osteoblast cells on the coating surface, which could contribute to the observed "good" biocompatibility of the nano TiO_2 coating. However, further work is required to produce experimental evidence to prove this hypothesis.

Other authors have also explored this possibility of creating nanostructures on the surface of TiO_2 coatings for biomedical applications. Liu et al. also used nanostructured agglomerated TiO_2 powders to produced APS coatings exhibiting nanostructures at the surface [87]. The surfaces of these coatings were plasma-treated (after coating deposition) by hydrogen ion implantation. It was observed that (i) a hydrogenated surface gave rise to negatively charged functional groups on the surface and (ii) the nanostructured zones (smaller than 50 nm) at the surface were crucial for the growth of apatite (due to surface adsorption) after immersion in simulated body fluid (SBF). Submicron agglomerated TiO_2 particles were also plasma sprayed. These coatings were also plasma-treated using the same approach of the nanostructured materials; however, apatite growth was not observed on the surface of these coatings. Therefore the presence of nanozones on the coating surface was important for this enhanced bioactivity of the nano TiO_2 coating.

Zhao et al., using the same type of nano TiO_2 coatings, also observed the growth of apatite after coating immersion in SBF [88]. However, instead of using a plasma treatment to activate the surface, a chemical method based on sodium hydroxide solutions was employed. It is clear that more extensive studies are required to investigate the in vivo performance of these various nanostructured titania coatings. However, the work to this point indicates that they hold promise as an interesting alternative to HA coatings.

6. Other Characteristics Observed for Nanostructured Ceramic Coatings

6.1 Deposition Efficiency

It has been observed by some researchers that the deposition efficiency (DE) values of nanostructured ceramic agglomerated powders are higher than those of conventional powders. Chen et al. observed for a series of four different plasma power

levels, DE values for nano YSZ of from 1.2 to 2 times higher than those for conventional YSZ (fused and crushed) [25]. For the same power, but three different spraying distances the DE of the nano YSZ was approximately 1.2 times higher.

Also for YSZ, Li et al. observed that the optimal DE of the nanopowder was 1.4 times higher than that of the optimal DE for the conventional material (HOSP) [24]. Ctibor et al. using water stabilized plasma (WSP) observed that for a conventional TiO_2 powder (fused and crushed) the energy consumption for thermal spraying was 0.6 kW/kg, whereas, for the agglomerated nano TiO_2 feedstock it was 0.4 kW/kg [89].

When comparing the DE values of nanostructured and conventional (clad) Al_2O_3-13wt% TiO_2 powders, the DE values for the nanostructured material were on average 1.5 times higher than those of the conventional material [60].

One possible explanation for these higher DE values of nanopowders is based on the high surface area of the nanostructured agglomerated powders (Figs. 1, 3 and 13). This larger surface area may allow the absorption of higher amounts of thermal energy during the particle dwell time in the spray jet, facilitating the melting process at the particle surface, which would also serve to promote the adhesion/cohesion of the impinging particles at the substrate.

6.2 Homogeneity of the Nanostructured Ceramic Coatings

Ctibor et al. recently analyzed the mechanical properties of nanostructured and conventional (fused and crushed) TiO_2 coatings deposited by WSP via depth-sensing nanoindentation [90]. Depth-sensing nanoindentation is a very useful tool to investigate the scatter in the values of the mechanical properties of materials. Due to the nature of the thermal spray process, coatings produced by this technique typically contain a significant number of defects and are inhomogeneous, anisotropic and exhibit a large variability in properties. In the work of Ctibor et al, it was observed that the use of a nanostructured feedstock reduced the probability of major defects, producing a more uniform microstructure. Despite the fact that the average values of hardness and elastic modulus of nanostructured and conventional TiO_2 were very similar, the nanostructured coating exhibited higher reliability. These observations may help to explain the superior

mechanical performance of nano TiO_2 coatings observed by other researchers [10, 43, 44]. The mechanisms by which the nanostructured feedstock promotes higher homogeneity have still yet to be explained.

7. The Future of Nanostructured Ceramic Thermal Spray Coatings

7.1 Challenges

The area of nanostructured thermal spray coatings is still relatively immature and no significant markets have yet been developed for these materials. Normally, the processing routes used to produce nanostructured powders are somewhat more sophisticated and time-consuming than those currently employed for manufacturing conventional feedstock materials. This results in higher product costs for nanostructured feedstock as compared to conventional powders. This is particularly true for conventional fused and crushed material. An additional consideration is the fact that many of these nanostructured materials are still being produced in relatively small quantities, which tends to keep the powder costs elevated. These costs should decrease as applications are identified and markets are penetrated, requiring higher volume production. Of course in terms of coating production, the fact that higher deposition efficiencies are often obtained with these nanostructured materials must be included when determining overall cost. Apart from the initial powder costs, which are often a major consideration when attempting to penetrate an existing market and displace a low-cost conventional powder, the benefits gained from using nanostructured coatings must be considered. Improved performance and/or longer life may lead to a substantial reduction in the overall cost, providing nanostructured coatings with a performance-to-cost advantage as compared to conventional coatings. Therefore, development in this field may progress by first penetrating niche markets. In addition to the challenges related to cost and market penetration, there is still much research, development and testing required in order to better understand the origin of improved performance. Aspects ranging from purity, nanoparticle size, and agglomerate size and distribution of the nanostructured feedstock powders to the role of the nanozones in enhancing the coating properties and affecting the

mechanisms that lead to improved performance must be investigated. This will not only lead to a better understanding of the various processes, it will also provide information that may enable further improvements in engineering nanostructured powders and coatings.

7.2 Success Stories

Anti-wear thermal spray coatings produced from nanostructured ceramic agglomerated powders are currently in use on parts employed by the U.S. Navy [91]. The choice of a nanostructured material for anti-wear applications was based on knowledge gained in earlier developmental work [6, 7, 35, 37-39]. The specific application involves the use of APS nanostructured Al_2O_3-13wt% TiO_2 coatings applied on the main propulsion shaft of ships. These shafts suffered from severe abrasion on the bearing surfaces, causing frequent and costly repairs. The use of conventional ceramic coatings was not considered feasible due to the high levels of torque, bending and fatigue experienced by these pieces, which normally would lead to failure of these conventional thermal spray coatings. However, due its known high toughness, the nanostructured Al_2O_3-13wt% TiO_2 ceramic coating was applied on the propulsion shafts of several U.S. Navy ships. One of these ships was inspected for any signs of coating wear after 3 months in operation. No visual signs of wear were detected. After four years in service, the ship was inspected again and no significant wear or delamination was recorded [91].

Nanostructured TiO_2 thermal spray coatings, developed by Perpetual Technologies (Ile des Soeurs, QC, Canada) [92], also have been employed commercially with success [43, 91]. A high pressure acid leach hydrometallurgical process employs autoclaves, valves and piping in a severe high temperature acidic slurry environment. Temperatures of 260°C, highly corrosive sulfuric acid (>95%), pressures up to 5500 kPa (~800 psi) and relatively high solids content (>20%wt.) can cause significant damage to the components, leading to problems of durability and profitability. Cr_2O_3-blend thermal spray coatings were applied on these ball valves, however, the low longevity of these coatings in service was significantly affecting the total plant costs. In order to perform a comparison, nano TiO_2 and conventional Cr_2O_3-blend thermal spray coatings were

deposited on the ball valves and put into service, and they were subsequently visually inspected after 10 months of use. The ball valve coated with Cr_2O_3-blend exhibited a high degree of coating delamination, whereas, the one coated with nano TiO_2 exhibited only a few regions of coating delamination and was put back into service [91].

8. Conclusions

The following conclusions can be drawn for thermal spray coatings engineered from nanostructured ceramic agglomerated powders (for anti-wear, abradable, TBC and biomedical applications) based on the work carried out at the National Research Council of Canada (NRC) since 2001 and the results of various other researchers working at different institutions working on the same subject.

8.1 Nanostructured Feedstock

- Nanostructured ceramic agglomerated feedstock powders are formed by spray-drying and sintering individual nanosized ceramic particles.
- The agglomerates are microscopic (to be employed in regular powder feeders) and normally porous.

8.2 Coating Microstructure

- Thermal spray coatings engineered from nanostructured agglomerated ceramic powders exhibit a bimodal microstructure, formed by particles that were fully molten and semi-molten in the spray jet.
- The semi-molten particles (i.e., nanozones) are found spread throughout the coating microstructure, including at the coating/substrate interface and coating surface.
- The nanozones can be dense or porous. Dense nanozones probably occur when the molten part of a semi-molten particle fully infiltrates into the capillaries of the

agglomerates during thermal spraying. When this infiltration is more limited, porous nanozones are formed.

- By engineering the amount and distribution of dense and porous nanozones, thermal spray coatings will exhibit radically different mechanical behaviors.

8.3 Anti-Wear Coatings

- Many researchers from different institutions have reported superior wear performance of nanostructured ceramic coatings (Al_2O_3, Al_2O_3-13wt% TiO_2, Al_2O_3-3wt% TiO_2, TiO_2 and YSZ) when compared to that of conventional coatings.
- The reduction in wear levels by employing nanostructured coatings (as compared to conventional coatings) can vary from 21% to 75% when the coatings are produced using the same torch. However, by employing HVOF and nanoceramics, the wear levels can be reduced by up to ~90% in comparison with the wear performance of optimized APS conventional ceramic coatings. Spraying ceramics via HVOF is a challenge, nonetheless, the wear performance of HVOF-sprayed nanostructured ceramics seems to be unmatched by that of APS conventional ceramics.
- The amount of nanozones embedded in the coating microstructure in order to produce an optimal wear performance varies from 11% to 25%. If the levels of these nanozones are above or below the ideal value (range) the optimal mechanical behavior is not produced.
- It is generally observed that the nanostructured coatings are not harder than the conventional ones, however, they tend to be much tougher. One of the hypothesis employed to explain this enhanced toughness (with some level of experimental evidence) is based on the crack arresting effect of the dense nanozones spread in the coating microstructure. This same hypothesis is employed to explain the better bond strength observed for some nanostructured coatings. Another hypothesis to explain the same behavior (with some level of experimental evidence) is based on

a better splat-to-splat contact achieved when using a nanostructured powder, which would also tend to impede crack propagation.

- The wear scars of nanostructured ceramic coatings tend to be smoother than those of conventional coatings. This may be an indication that the nanocoatings are easier to grind and polish.

8.4 Abradable Ceramic Coatings

- By spraying nanostructured agglomerated ceramic powders it is possible to engineer ceramic abradable coatings targeted for use in the high temperature environments of gas turbines. These coatings can be considered as the opposite of anti-wear coatings.
- In order to engineer a friable ceramic coating, the molten part of a semi-molten agglomerate particle can not fully infiltrate into the capillaries of its non-molten core during thermal spraying.
- The porous nanozones spread throughout the coating microstructure will act as weak links, thereby making the coating friable.
- During rub-rig testing, nanostructured ceramic coatings can exhibit a similar behavior to that of a metallic-based abradable coating.
- The amount of porous nanozones embedded in the coating microstructure in order to produce abradability levels similar to those of metallic-based abradables is found within the range of 30%-35%.

8.5 TBCs

- Researchers have measured the thermal diffusivity of nanostructured and conventional YSZ coatings up to temperatures of 1200°C (heating and cooling steps). The thermal diffusivity of the nanostructured YSZ coating was found to be lower throughout the experiment.
- Researchers have performed thermal shock tests to evaluate the performance of nano and conventional YSZ coatings. The thermal shock resistance of the nano

YSZ coating is 2-4 times higher than that of the conventional material. The high toughness of the nanostructured coatings may have played an important role in these results, however, no strong experimental evidence was shown.

- High temperature exposure leads to an increase of the size of the particles located at the nanozones. The nanoporosity contained in the nanozones tends to be healed.
- Creep measurements indicated that the higher creep rate of the nano YSZ coatings would result in an enhanced relaxation during stress at elevated temperatures, which is a desirable phenomenon. On the other hand, this enhanced relaxation at high temperatures may lead to the development of stresses during cooling, which may lead to a premature failure of the coating. However, the thermal shock tests reported in the literature up to this point show positive results for the nanocoatings.

8.6 Biomedical Coatings

- Up to this point it has been shown that nanostructured HA coatings do not exhibit superior mechanical behavior when compared to conventional HA coatings. The reason for this characteristic may lie in the inherent low mechanical performance of the HA material.
- It was demonstrated by using an osteoblast cell culture (in vitro) that the type of HA coating phase is more important than the nanostructural character of the coating, however, HA coatings with a high content of both crystalline HA and nanostructures were preferred for cell proliferation.
- HVOF-sprayed nano TiO_2 coatings have demonstrated bond strength values at least 2.4 times higher than those of HA coatings on Ti-6Al-4V substrates. Preliminary in vitro tests indicated that these coatings have also demonstrated at least equivalent (or maybe higher) biocompatibility levels when compared to those of conventional HA coatings. In vivo tests (with rabbits) demonstrated that these coatings (deposited on Ti-6Al-4V substrates) have a higher degree of bone apposition when compared to that of uncoated Ti-6Al-4V substrates.

- Based on cell culture (in vitro) results found for bulk nanostructured ceramics, the nanostructured TiO_2 zones found on this coating surface may have played an important role producing these good biocompatibility results (due to biomimetism with adhesion proteins), however, up to this point there is no experimental evidence to prove this.
- APS nano TiO_2 coatings, exhibiting nanostructural character at the surface, can be plasma or chemically treated to allow the deposition of apatite on their surfaces during immersion in SBF. It is claimed that the nanozones on the coating enhanced its capacity of surface adsorption, therefore facilitating the growth of apatite. It is important to mention that the growth of apatite was not observed for other TiO_2 coatings engineered without a strong nanostructural character at their surfaces.
- Based on these findings it may be stated that nano TiO_2 coatings may become in the future an interesting alternative to HA coatings for biomedical applications.

8.7 Deposition Efficiency

- Nanostructured ceramic agglomerated powders tend to exhibit higher DE levels (from 1.2 to 2 times higher) when compared to those of conventional materials.
- The high DE performance may be related to the high surface area available for the nanostructured particles, which would allow them to absorb higher amounts of thermal energy while in the spray jet.

Acknowledgments

This research on nanostructured ceramic thermal spray coatings carried out at the NRC since 2001 could not have been done without the very important assistance of the following technicians: J. –F. Alarie and E. Poirier (metallography and mechanical testing), S. Bélanger (air plasma spraying), F. Belval (HVOF spraying), B. Harvey (spray booth engineering), M. Lamontagne (in-flight particle measurements of temperature and

velocity) and M. Thibodeau (microscopy and XRD). Their efforts and commitment towards the accomplishment this work are deeply appreciated.

References

1. C. C. Koch, Nanostructured Materials – Processing, Properties, and Applications, Noyes Publications, William Andrew Publishing, Norwich, NY, USA, 2002.

2. Y. Lu, P. K. Liaw, The Mechanical Properties of Nanostructured Materials, Journal of Metals, Vol. 53, No. 3, March, 2001, p 31-35.

3. S. Iijima, Helical Microtubules of Graphitic Carbon, Nature, Vol. 354, 1991, p 56-58.

4. R. S. Lima, B. R. Marple, Superior Performance of High-Velocity Oxyfuel-Sprayed Nanostructured TiO_2 in Comparison to Air Plasma-Sprayed Conventional Al_2O_3-13TiO_2, Journal of Thermal Spray Technology. 14(3), 2005, p 397-404.

5. L. L. Shaw, D. Goberman, R. Ren, M. Gell, S. Jiang, Y. Wang, T. D. Xiao, P. R. Strutt, The Dependency of Microstructure and Properties of Nanostructured Coatings on Plasma Spray Conditions, Surface and Coatings Technology, 130, 2000, p 1-8.

6. Y. Wang, S. Jiang, M. Wang, S. Wang, T. D. Xiao, P. R. Strutt, Abrasive Wear Characteristics of Plasma Sprayed Nanostructured Alumina/Titania Coatings, Wear, 237, 2000, p 176-185.

7. E. H. Jordan, M. Gell, Y. H. Sohn, D. Goberman, L. Shaw, S. Jiang, M. Wang, T. D. Xiao, Y. Wang, P. Strutt, Fabrication and Evaluation of Plasma Sprayed Nanostructured Alumina-Titania Coatings with Superior Properties, Materials Science and Engineering A, 301, 2001, p 80-89.

8. R. S. Lima, A. Kucuk, C. C. Berndt, Evaluation of Microhardness and Elastic Modulus of Thermally Sprayed Nanostructured Zirconia Coatings, Surface and Coatings Technology, 135, 2001, p 166-172.

9. R. S. Lima, A. Kucuk, C. C. Berndt, Integrity of Nanostructured Partially Stabilized Zirconia After Plasma Spray Processing, Materials Science and Engineering A, 313, 2001, p 75-82.

10. R. S. Lima, B. R. Marple, Enhanced Ductility in Thermally Sprayed Titania Coating Synthesized Using a Nanostructured Feedstock, Materials Science and Engineering A, 395, 2005, p 269-280.

11. Inframat Corp., www.inframat.com, July 26, 2006.

12. Altair Nanomaterials Inc., www.altairnano.com, July 26, 2006.

13. Millidyne Surface Technologies, www.millidyne.fi, July 26, 2006 (*in Finnish*).

14. Y. Zeng, S. W. Lee, L. Gao, C. X. Ding, Atmospheric Plasma Sprayed Coatings of Nanostructured Zirconia, Journal of the European Ceramic Society, 22, 2002, p 347-351.

15. R. S. Lima, K. A. Khor, H. Li, P. Cheang, B. R. Marple, HVOF Spraying of Nanostructured Hydroxyapatite for Biomedical Applications, Materials Science and Engineering A, 396, 2005, p 181-187.

16. E. Turunen, T. Varis, T. E. Gustafsson, J. Keskinen, T. Falt, S. -P. Hannula, Parameter Optimization of HVOF Sprayed Nanostructured Alumina and Alumina-Nickel Composite Coatings, Surface and Coatings Technology, 200, 2006, p 4987-4994.

17. H. Chen, Y. Zhang, C. Ding, Tribological Properties of Nanostructured Zirconia Coatings Deposited by Plasma Spraying, Wear, 253, 2002, p 885-893.

18. Y. Zeng, S. W. Lee, C. X. Ding, Plasma Spray Coatings in Different Nanosize Alumina, Materials Letters, 57, 2002, p 495-501.

19. H. Chen, C. X. Ding, Nanostructured Zirconia Coating Prepared by Atmospheric Plasma Spraying, Surface and Coatings Technology, 150, 2002, p 31-36.

20. H. Chen, C. Ding, S. Lee, Phase Composition and Microstructure of Vacuum Plasma Sprayed Nanostructured Zirconia Coating, Materials Science and Engineering A, 361, 2003, p 58-66.

21. H. Chen, C. Ding, P. Zhang, P. La, S. W. Lee, Wear of Plasma-Sprayed Nanostructured Zirconia Coatings Against Stainless Steel Under Distilled-Water Conditions, Surface and Coatings Technology, 173, 2003, p 144-149.

22. H. Chen, Y. Zeng, C. Ding, Microstructural Characterization of Plasma-Sprayed Nanostructured Zirconia Powders and Coatings, Journal of the European Ceramic Society, 23, 2003, p 491-497.

23. H. Chen, X. Zhou, C. Ding, Investigation of the Thermomechanical Properties of a Plasma-Sprayed Nanostructured Zirconia Coating, Journal of the European Ceramic Society, 23, 2003, p 1449-1455.

24. J. F. Li, H. Liao, X. Y. Wang, B. Normand, V. Ji, C. X. Ding, C. Coddet, Improvement in Wear Resistance of Plasma Sprayed Yttria Stabilized Zirconia Coating Using Nanostructured Powder, Tribology International, 37, 2004, p 77-84.

25. H. Chen, S. W. Lee, H. Du, C. X. Ding, C. H. Choi, Influence of Feedstock and Spraying Parameters on the Depositing Efficiency and Microhardness of Plasma-Sprayed Zirconia Coatings, Materials Letters, 58, 2004, p 1241-1245.

26. B. Liang, C. Ding, Thermal Shock Resistances of Nanostructured and Conventional Zirconia Coatings Deposited by Atmospheric Plasma Spraying, Surface and Coatings Technology, 197, 2005, p 185-192.

27. B. Liang, C. Ding, Phase Composition of Nanostructured Zirconia Coatings Deposited by Air Plasma Spraying, Surface and Coatings Technology, 191, 2005, p 267-273.

28. W. Q. Wang, C. K. Sha, D. Q. Sun, X. Y. Gu, Microstructural Feature, Thermal Shock Resistance and Isothermal Oxidation Resistance of Nanostructured Zirconia Coating, Materials Science and Engineering A, 424, 2006, p 1-5.

29. B. Liang, C. Ding, H. Liao, C. Coddet, Phase Composition and Stability of Nanostructured 4.7wt% Yttria-Stabilized Zirconia Coatings Deposited by Atmospheric Plasma Spraying, Surface and Coatings Technology, 200, 2006, p 4549-4556.

30. X. Lin, Y. Zeng, X. Zhou, C. Ding, Microstructure of Alumina-3wt% Titania Coatings by Plasma Spraying with Nanostructured Powders, Materials Science and Engineering A, 357, 2003, p 228-234.

31. X. Lin, Y. Zeng, S. W. Lee, C. Ding, Characterization of Alumina-3wt% Titania Coating Prepared by Plasma Spraying of Nanostructured Powders, Journal of the European Ceramic Society, 24, 2004, p 627-634.

32. B. Liang, H. Liao, C. Ding, C. Coddet, Nanostructured Zirconia-30vol% Alumina Composite Coatings Deposited by Atmospheric Plasma Spraying, Thin Solid Films, 484, 2005, p 225-231.

33. J. Ahn, B. Hwang, E. P. Song, S. Lee, N. J. Kim, Correlation of Microstructure and Wear Resistance of Al_2O_3-TiO_2 Coatings Plasma Sprayed with Nanopowders, Matallurgical and Materials Transactions A, Vol. 37A, June, 2006, p 1851-1861.

34. E. P. Song, J. Ahn, S. Lee, N. J. Kim, Microstructure and Wear Resistance of Nanostructured Al_2O_3-8wt% TiO_2 Coatings Plasma-Sprayed with Nanopowders, Surface and Coatings Technology, *in press*.

35. M. Gell, E. H. Jordan, Y. H. Sohn, D. Goberman, L. Shaw, T. D. Xiao, Development and Implementation of Plasma Sprayed Nanostructured Ceramic Coatings, Surface and Coatings Technology, 146-147, 2001, p 48-54.

36. R. S. Lima, A. Kucuk, C. C. Berndt, Bimodal Distribution of Mechanical Properties on Plasma Sprayed Nanostructured Partially Stabilized Zirconia, Materials Science and Engineering A, 327, 2002, p 224-232.

37. D. Goberman, Y. H. Sohn, L. Shaw, E. Jordan, M. Gell, Microstructure Development of Al_2O_3-13wt% TiO_2 Plasma Sprayed Coatings Derived from Nanocrystalline Powders, Acta Materialia, 50, 2002, p 1141-1152.

38. H. Luo, D. Goberman, L. Shaw, M. Gell, Indentation Fracture Behavior of Plasma-Sprayed Nanostructured Al_2O_3-13wt% TiO_2 Coatings, Materials Science and Engineering A, 346, 2003, p 237-245.

39. P. Bansal, N. P. Padture, A. Vasiliev, Improved Interfacial Mechanical Properties of Al_2O_3-13wt% TiO_2 Plasma-Sprayed Coatings Derived from Nanocrystalline Powders, Acta Materialia, 51, 2003, p 2959-2970.

40. R. S. Lima, B. R. Marple, A. Dadouche, W. Dmochowski, B. Liko, Nanostructured Abradable Coatings for High Temperature Applications, PDF file in Proceedings of the International Thermal Spray Conference 2006, Eds. B. R. Marple, M. M. Hyland, Y. –C. Lau, R. S. Lima, J. Voyer, ASM International, Materials Park, OH, USA, 2006.

41. K. Muraleedharan, J. Subrahmanyam, and S.B. Bhaduri, Indentification of t' Phase in ZrO_2-7.5wt% Y_2O_3 Thermal-Barrier Coatings, Journal of the American Ceramic Society, Vol 71 (No. 5), 1988, p C-226-227.

42. S. Tao, B. Liang, C. Ding, H. Lao, C. Coddet, Wear Characteristics of Plasma-Sprayed Nanostructured Yttria Partially Stabilized Zirconia Coatings, Journal of Thermal Spray Technology, Vol. 14, No. 4, 2005, p 518-523.

43. G. E. Kim, J. Walker Jr., J. B. Williams Jr., Nanostructured Titania Coated Titanium, US Patent 6,835,449 B2, December 28, 2004.

44. R. S. Lima, B. R. Marple, From APS to HVOF Spraying of Conventional and Nanostructured Titania Feedstock Powders: a Study on the Enhancement of the Mechanical Properties, Surface and Coatings Technology, 200, 2000, p 3428-3437.

45. Y. Liu, T. E. Fischer, A. Dent, Comparison of HVOF and Plasma-Sprayed Alumina/Titania Coatings – Microstructure, Mechanical Properties and Abrasion Behavior, Surface and Coatings Technology, 167 (2003) p 68-76.

46. R. S. Lima, H. Li, K. A. Khor, B. R. Marple, Biocompatible Nanostructured High Velocity Oxy-Fuel Sprayed Titania Coating: Deposition, Characterization and Mechanical Properties, Journal of Thermal Spray Technology, accepted for publication.

47. N. Berger-Keller, G. Bertrand, C. Filiare, C. Meunier, C. Coddet, Microstructure of Plasma-Sprayed Titania Coatings Deposited from Spray-Dried Powder, Surface and Coatings Technology, 168, 2003, p 281-290.

48. G. R. Anstis, P. Chantikul, B. R. Lawn, D. B. Mashall, A Critical Evaluation of Indentation Techniques for Measuring Fracture Toughness: I. Direct Crack Measurements, Journal of the American Ceramic Society, Vol. 64, No. 9, 1981, p 1073-1082.

49. R. McPherson, A Review of Microstructure and Properties of Plasma Sprayed Ceramic Coatings, Surface and Coatings Technology, 39/40, 1989, p 173-181.

50. P. Ostojic, R. McPherson, Indentation Toughness Testing of Plasma Sprayed Coatings, Materials Forum, Vol. 10, No. 4, 1987, p 247-255.

51. H. Chen, S. Lee, X. Zheng, C. Ding, Evaluation of Unlubricated Wear Properties of Plasma-Sprayed Nanostructured and Conventional Zirconia Coatings by SRV Tester, Wear, 260, 2006, p 1053-1060.

52. Standard Test Method for Adhesion or Cohesion Strength of Thermal Spray Coatings, ASTM Standard C 633-01, ASTM, West Conshohocken, PA, USA.

53. X. Liu, B. Zhang, Z. Deng, Grinding Nanostructured Ceramic Coatings: Surface Observation and Material Removal Mechanisms, International Journal of Machine Tools & Manufacture, 42, 2002, p 1665-1676.

54. X. Liu, B. Zhang, Grinding of Nanostructural Ceramic Coatings: Damage Evaluation, International Journal of Machine Tools & Manufacture, 43, 2003, p 161-167.

55. R. S. Lima, B. R. Marple, High Weibull Modulus HVOF Titania Coatings, Journal of Thermal Spray Technology, 12(2), 2003, p 240-249.

56. R. S. Lima, B. R. Marple, Optimized HVOF Titania Coatings, Journal of Thermal Spray Technology, 12(3), 2003, p 360-369.

57. A. Kulkarni, J. Gutleber, S. Sampath, A. Goland, W. B. Lindquist, H. Herman, A. J. Allan, B. Dowd, Materials Science and Engineering A, 369, 2004, p 124-137.

58. E. Turunen, T. Varis, S. –P. Hannula, A. Vaidya, A. Kulkarni, J. Gutleber, S. Sampath, H. Herman, On the Role of Particle State and Deposition Procedure on Mechanical, Tribological and Dielectric Response of High Velocity Oxy-Fuel Sprayed Alumina Coatings, Materials Science and Engineering A, 415, 2006, p 1-11.

59. A. Ibrahim, R. S. Lima, B. R. Marple, C. C. Berndt, Fatigue and Mechanical Properties of Nanostructured versus Conventional Titania (TiO_2) Coatings, PDF copy in Proceedings of the International Thermal Spray Conference 2005, DVS-Verlag GmbH, Dusseldorf, Germany, 2004.

60. R. S. Lima, C. Moreau, B. R. Marple, HVOF-Sprayed Nanostructured Al_2O_3-TiO_2 Coatings: An Enhanced Wear Performance, Proceedings of the International Thermal Spray Conference 2007, to be submitted.

61. M. O. Borel, A. R. Nicoll, H. W. Schlapfer, R. K. Schmid, The Wear Mechanisms Occuring in Abradable Seals of Gas Turbines, Surface and Coatings Technology, Vol. 39/40, 1989, p 117-126.

62. Y. Nava, Z. Mutasim, and M. Coe, Ceramic Abradable Coatings for Applications up to 1100°C, Thermal Spray 2001: New Surfaces for a New Millenium, Eds. C. C. Berndt, K. A. Khor, E. F. Lugscheider, ASM International, Materials Park, OH, USA, 2001, p 119-126.

63. F. Ghasripoor, R. Schmid, and M. Dorfman, Abradable Coatings Increase Gas Turbine Efficiency, *Materials World*, Vol 5 (No. 6), 1997, p 328-330.

64. T. A. Taylor, Thermal Properties and Microstructure of Two Thermal Barrier Coatings, Surface and Coatings Technology, 54/55, 1992, p 53-57.

65. R. E. Taylor, X. Wang, X. Xu, Thermophysical Properties of Thermal Barrier Coatings, Surface and Coatings Technology, 120-121, 1999, p 89-95.

66. N. Wang, C. Zhou, S. Gong, H. Xu, Heat Treatment of Nanostructured Thermal Barrier Coatings, Ceramics International, *in press*.

67. O. Racek, C. C. Berndt, D. N. Guru, J. Heberlein, Nanostructured and Conventional YSZ Coatings Deposited Using APS and TTPR Techniques, Surface and Coatings Technology, 201, 2006, p 338-346.

68. R. Soltani, E. Garcia, T. W. Coyle, J. Mostaghimi, R. S. Lima, B. R. Marple, C. Moreau, Thermo-Mechanical Behavior of Nanostructured Plasma Sprayed Zirconia Coatings, Journal of Thermal Spray Technology, accepted for publication.

69. T. J. Webster, R. W. Siegel, R. Bizios, Osteoblast Adhesion on Nanophase Ceramics, Biomaterials, 20, 1999, p 1221-1227.

70. L. G. Gutwein, T. J. Webster, Increased Viable Osteoblast Density in the Presence of Nanophase Compared to Conventional Alumina and Titania Particles, Biomaterials, 25, 2004, p 4175-4183.

71. T. J. Webster, C. Ergun, R. H. Doremus, R. W. Siegel, R. Bizios, Specific Proteins Mediate Enhanced Osteoblast Adhesion on Nanophase Ceramics, Journal of Biomedical Materials Research, 51(3), 2000, p 475-483.

72. T. J. Webster, C. Ergun, R. H. Doremus, R. W. Siegel, R. Bizios, Enhanced Functions of Osteoblasts on Nanophase Ceramics, Biomaterials, 21, 2000, p 1803-1810.

73. H. P. Erickson, N. Carrell, J. McDonagh, Fibronectin Molecule Visualized in Electron Microscopy: A Long, Thin, Flexible Strand, The Journal of Cell Biology, 91, 1981, p 673-678.

74. R. McPherson, N. Gane, T. J. Bastow, Structural Characterization of Plasma-Sprayed Hydroxyapatite Coatings, Journal of Materials Science: Materials in Medicine, 6, 1995, p 327-334.

75. H. Li, K. A. Khor, Characteristics of the Nanostructures in Thermal Sprayed Hydroxyapatite Coatings and Their Influence on Coating Properties, Surface and Coatings Technology, *in press*.

76. Y. C. Yang, C. Chang, The Bonding of Plasma-Sprayed Hydroxyapatite Coatings to Titanium: Effect of Processing, Porosity and Residual Stress, Thin Solid Films, 444, 2003, p 260-275.

77. H. Li, K. A. Khor, P. Cheang, Effect of the Powders' Melting State on the Properties of HVOF Sprayed Hydroxyapatite Coatings, Materials Science and Engineering A, 293, 2000, p 71-80.

78. L. I. Havelin, B. Espehaug, L. B. Engesaeter, The Performance of Two Hydroxyapatite-Coated Acetabular Cups Compared with Charnley Cups, Journal of Bone and Joint Surgery (Br), Vol 84-B (No. 6), 2002, p 839-845.

79. O. Reikeras, R. B. Gunderson, Failure of HA Coating on a Gritblasted Acetabular Cup, Acta Orthop. Scand., Vol 73 (No. 1), 2002, p 104-108.

80. J. Blacha, High Osteolysis and Revision Rate with the Hydroxyapatite-Coated ABG Hip Prostheses, Acta Orthop. Scand., Vol. 75 (No.3), 2004, p 276-282.

81. K. A. Lai et al., Failure of Hydroxyapatite-Coated Acetabular Cups, Journal of Bone and Joint Surgery (Br), Vol 84-B (No. 5), 2002, p 641-646.

82. S. Overgaard, K. Soballe, K. Josephsen, E. S. Hansen, and C. Bunger, Role of Different Loading Conditions on Resorption of Hydroxyapatite Coating Evaluated by Histomorphometric and Stereological Methods, J. Orthop. Res., Vol 14, 1996, p 888-894.

83. M. A. Lopes, F.J. Monteiro, and J. D. Santos, Glass-Reinforced Hydroxyapatite Composites: Fracture Toughness and Hardness Dependence on Microstructural Characteritics, Biomaterials, Vol 20, 1999, p 2085-2090.

84. M. Espagnol, V. Guipont, K. A. Khor, M. Jeandin, N. Llorca-Isern, Effect of Heat Treatment on High Pressure Plasma Sprayed Hydroxyapatite Coatings, Surface Engineering, Vol 18, No 3, 2002, p 213-218.

85. J. -G. Legoux, F. Chellat, R. S. Lima, B. R. Marple, M. N. Bureau, H. Shen, G. A. Candeliere, Journal of Thermal Spray Technology, accepted for publication.

86. B. R. Marple, R. S. Lima, H. Li, K. A. Khor, Biomimetic Ceramic Surfaces Produced by Thermal Spraying Nanostructured Titania: A Coating Alternative to Hydroxyapatite on Orthopedic Implants?, Key Engineering Materials, 309-311, 2006, p 739-742.

87. X. Liu, X. Zhao, R. K. Y. Fu, J. P. Y. Ho, C. Ding, P. K. Chu, Plasma-Treated Nanostructured TiO_2 Surface Supporting Biomimetic Growth of Apatite, Biomaterials, 26, 2005, p 6143-6150.

88. X. Zhao, X. Liu, C. Ding, P. K. Chu, In Vitro Bioactivity of Plasma-Sprayed TiO2 Coatings after Sodium Hydroxide Treatment, Surface and Coatings Technology, 200, 2006, p 5487-5492.

89. P. Ctibor, K. Neufuss, J. Dubsky, B. Kolman, P. Rohan, P. Chraska, Spraying of Agglomerated TiO_2 Nanopowder by Water-Stabilized Plasma, PDF file in Proceedings of the International Thermal Spray Conference 2006, Eds. B. R. Marple, M. M. Hyland, Y. –C. Lau, R. S. Lima, J. Voyer, ASM International, Materials Park, OH, USA, 2006.

90. P. Ctibor, P. Bohac, M. Stranyanek, R. Ctvrtlik, Structured and Mechanical Properties of Plasma Sprayed Coatings of Titania and Alumina, Journal of the European Ceramic Society, *in press*.

91. G. E. Kim, Proven and Promising Applications Thermal Sprayed Nanostructured Coatings, PDF file in Proceedings of the International Thermal Spray Conference 2006, Eds. B. R. Marple, M. M. Hyland, Y. –C. Lau, R. S. Lima, J. Voyer, ASM International, Materials Park, OH, USA, 2006.

92. Perpetual Technologies, www.perpetualtech.ca, August 10, 2006.

Table Titles

Figure Titles

Figure 1 – (a) Titania feedstock particle formed by the agglomeration (spray-drying) of individual nanosized particles of titania [4]. (b) Particle of (a) observed at higher magnification; individual nanosized titania particles smaller than 100 nm [4].

Figure 2 – Typical schematic (cross-section) of the bimodal microstructure of thermal spray coatings formed by fully molten and semi-molten nanostructured agglomerated particles.

Figure 3 – (a) YSZ feedstock particle formed by the agglomeration (spray-drying) of individual nanosized particles of YSZ [40]. (b) Particle of (a) observed at higher magnification showing individual nanosized YSZ particles (30-130 nm) [40].

Figure 4 - (a) Microstructure of the nanostructured zirconia-yttria coating made from a nanostructured feedstock (Fig. 3) [40]. (b) Darker-colored regions containing (c) the semi-molten feedstock particles [40].

Figure 5 – Cross-section of an HVOF-sprayed coating made from a conventional titania fused and crushed feedstock [10].

Figure 6 – (a) Cross-section of an HVOF-sprayed coating made from a nanostructured feedstock (Fig. 1) [10]. (b) High magnification view of (a) showing a semi-molten nanostructured feedstock particle embedded in the coating microstructure.

Figure 7 – Vickers indentation impression (5 kgf) and crack propagation in the cross-section of the HVOF-sprayed titania coating made from the conventional fused and crushed feedstock [10].

Figure 8 – (a) Vickers indentation impression (5 kgf) and crack propagation in the cross-section of the HVOF-sprayed titania coating made from the nanostructured feedstock (Fig. 1) [10]. (b) Vickers indentation crack tip arresting after passing through a nanozone in the nanostructured coating [10].

Figure 9 – SEM picture (taken at 50° angle) of the wear scar of an HVOF-sprayed nanostructured titania coating of Figs. 6 and 8 [10].

Figure 10 – SEM picture (taken at 50° angle) of the wear scar of an HVOF-sprayed conventional titania coating of Figs. 5 and 7 [10].

Figure 11 – Wear scar formed during rub-rig testing on the surface of nanostructured YSZ coating of Fig. 4 [40].

Figure 12 – Wear scar formed during rub-rig testing on the surface of CoNiCrAlY-BN-polyester abradable coating.

Figure 13 – (a) HA feedstock particle formed by the agglomeration (spray-drying) of individual nanosized particles of HA. (b) Particle of (a) observed at higher magnification; individual nanosized HA particles with widths smaller than 100 nm.

Figure 14 – Cross-section of an HVOF-sprayed HA coating made from a nanostructured feedstock (Fig. 13) [15].

Figure 15 – Different types of nanostructural characteristics found in the cross-section of the HA coating if Fig. 14. (a) porous, (b) fibrous [15] and (c) densely packed [15] nanozones.

Figure 16 – Osteoblast cell culture (7 day-incubation) on the surface of the HVOF-sprayed nano TiO_2 coating of Figs. 6 and 8.

Figure 17 – Osteoblast cell culture (7 day-incubation) on the surface of an APS conventional HA coating.

Figure 18 - Relative intensity of red staining (alkaline phosphatase activity) for the osteoblast cells on the surface of the HVOF-sprayed nano TiO_2 (Figs. 6 and 8) and APS conventional HA (Fig. 16) coatings after a 15-day cell culture. The percentage of the coating covered in red is a measure of the osteoblast cells' ability to adhere, proliferate, and differentiate on the coating surface.

Figure 19 – (a) (b) (c) Images of nanozones found on the as-sprayed surface of the HVOF-sprayed nano titania coating of Figs. 6 and 8.

Table 1 – Reduction in wear levels given by nanostructured coatings when the nanostructured and conventional powders are sprayed with the same type of thermal spray torch.

Coating	**Conventional feedstock**	**Reduction in wear levels by spraying a nanostructured feedstock**	**Reference**
YSZ	Sintered and crushed and HOSP	From 21% to 75%	17, 21, 24, 42, 50
Al_2O_3	Fused and crushed	32%	16
Al_2O_3-3wt% TiO_2	Fused and crushed	39%	31
Al_2O_3-13wt% TiO_2	Clad	From 71% to 75%	7, 33, 35
TiO_2	Fused and crushed	From 25% to 52%	10, 43

Table 2 – Reduction in wear levels obtained from spraying conventional ceramic powders via APS (traditional method) to spraying nanostructured ceramic powders via HVOF (alternative method).

Coating	**Conventional feedstock**	**Reduction in wear levels by spraying a nanostructured ceramic feedstock via HVOF**	**Reference**
TiO_2	Fused and crushed	~60%	44
Al_2O_3-13wt% TiO_2	Clad	~90%	60

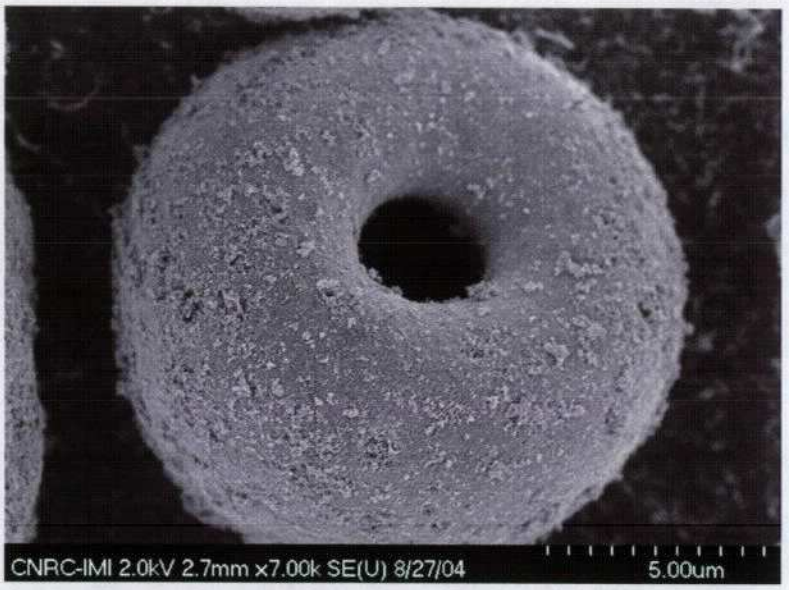

(a)

(b)

Figure 1 – (a) Titania feedstock particle formed by the agglomeration (spray-drying) of individual nanosized particles of titania [4]. (b) Particle of (a) observed at higher magnification; individual nanosized titania particles smaller than 100 nm [4].

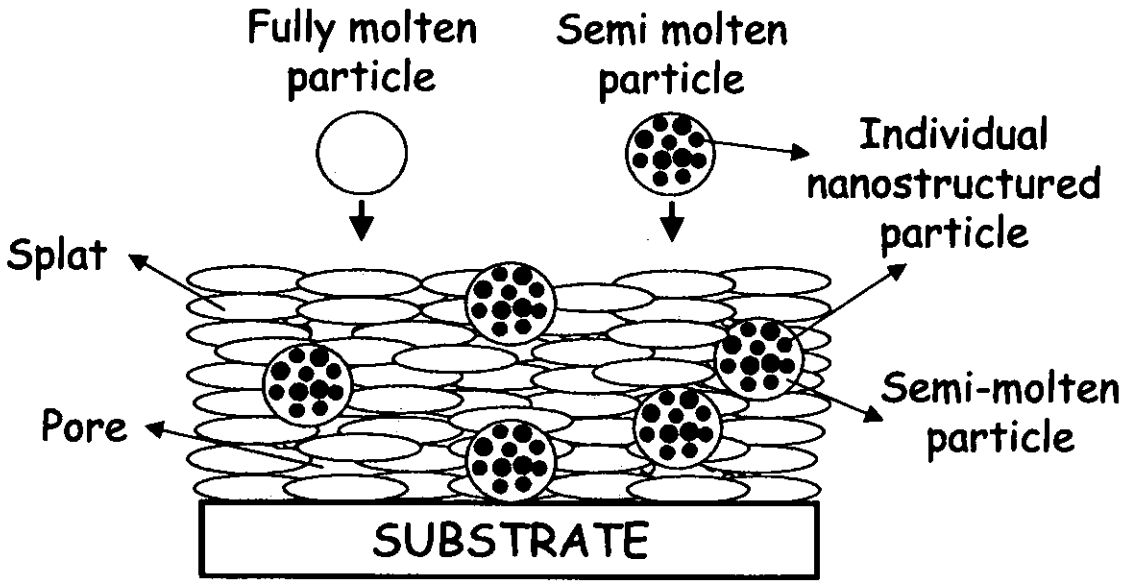

Figure 2 – Typical schematic (cross-section) of the bimodal microstructure of thermal spray coatings formed by fully molten and semi-molten nanostructured agglomerated particles.

(a)

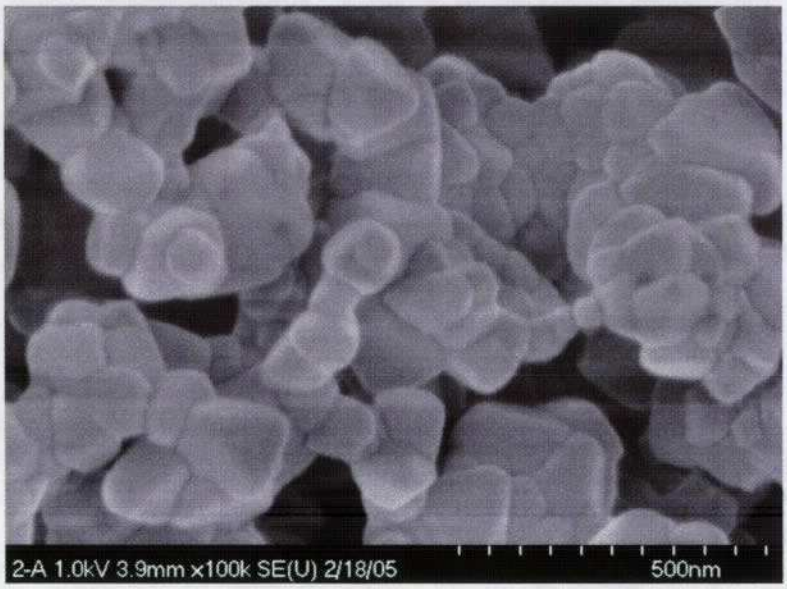

(b)

Figure 3 – (a) YSZ feedstock particle formed by the agglomeration (spray-drying) of individual nanosized particles of YSZ [40]. (b) Particle of (a) observed at higher magnification showing individual nanosized YSZ particles (30-130 nm) [40].

(a)

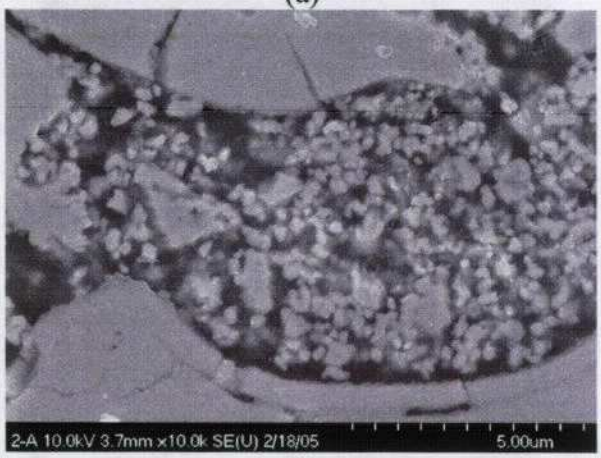

(b)

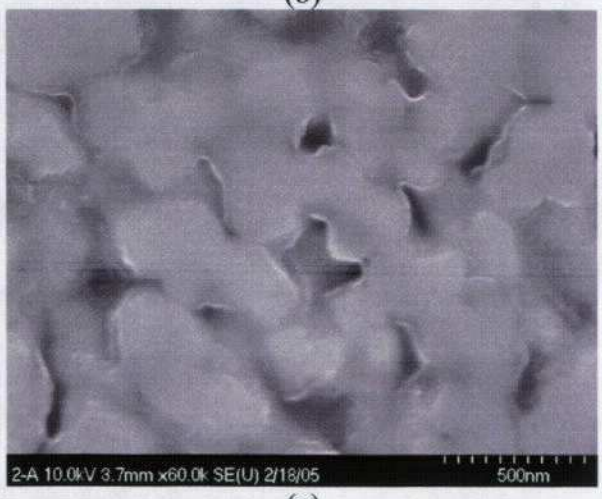

(c)

Figure 4 - (a) Microstructure of the nanostructured zirconia-yttria coating made from a nanostructured feedstock (Fig. 3) [40]. (b) Darker-colored regions containing (c) the semi-molten feedstock particles [40].

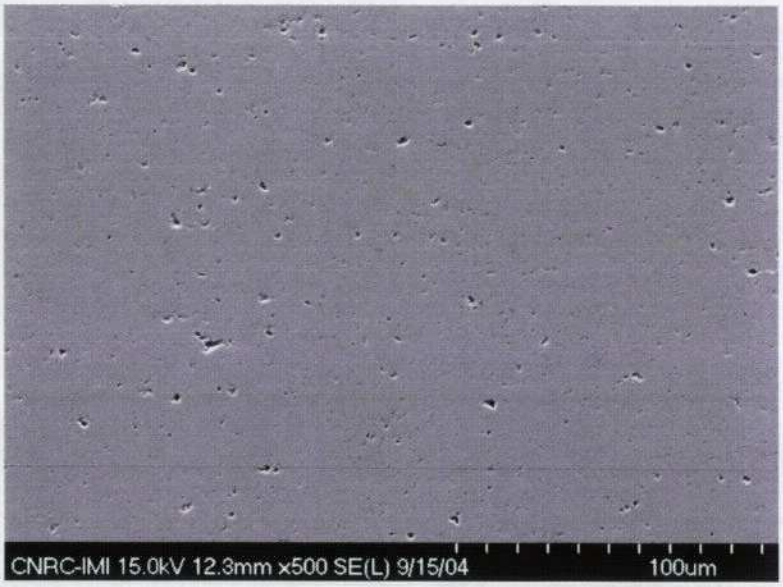

Figure 5 – Cross-section of an HVOF-sprayed coating made from a conventional titania fused and crushed feedstock [10].

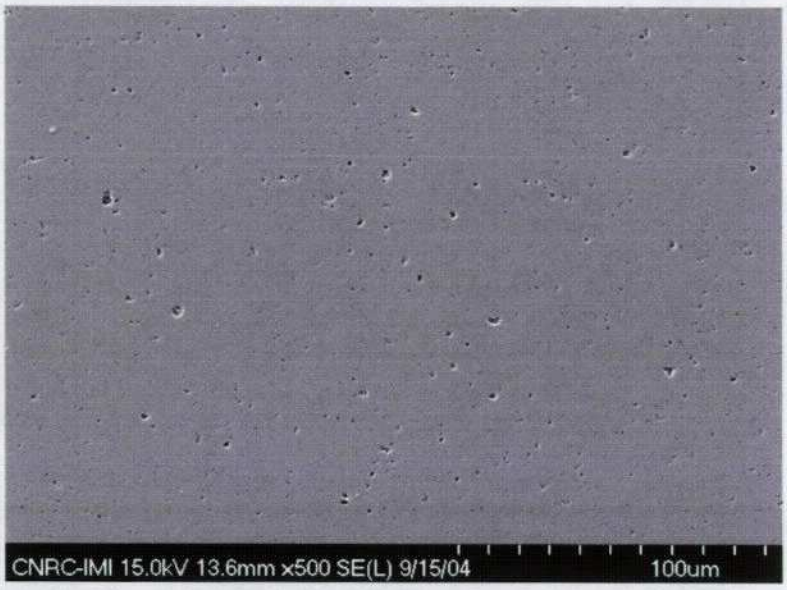

(a)

(b)

Figure 6 – (a) Cross-section of an HVOF-sprayed coating made from a nanostructured feedstock (Fig. 1) [10]. (b) High magnification view of (a) showing a semi-molten nanostructured feedstock particle embedded in the coating microstructure.

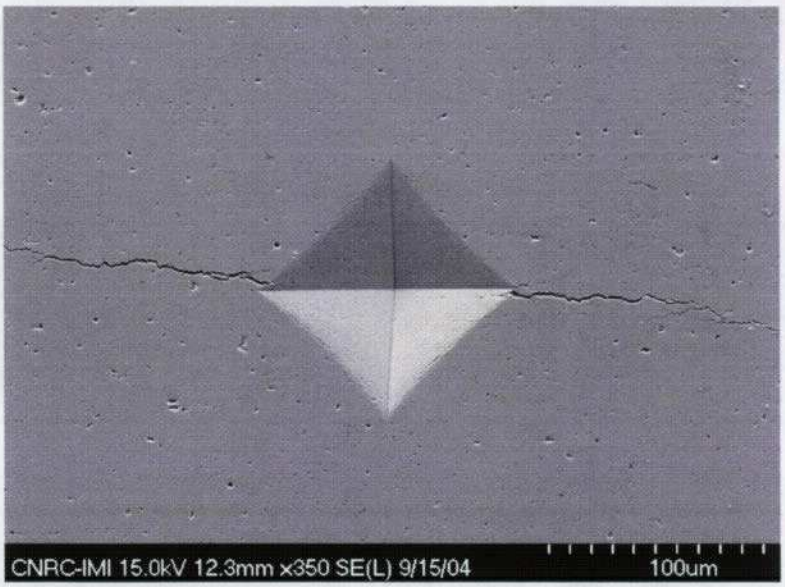

Figure 7 – Vickers indentation impression (5 kgf) and crack propagation in the cross-section of the HVOF-sprayed titania coating made from the conventional fused and crushed feedstock [10].

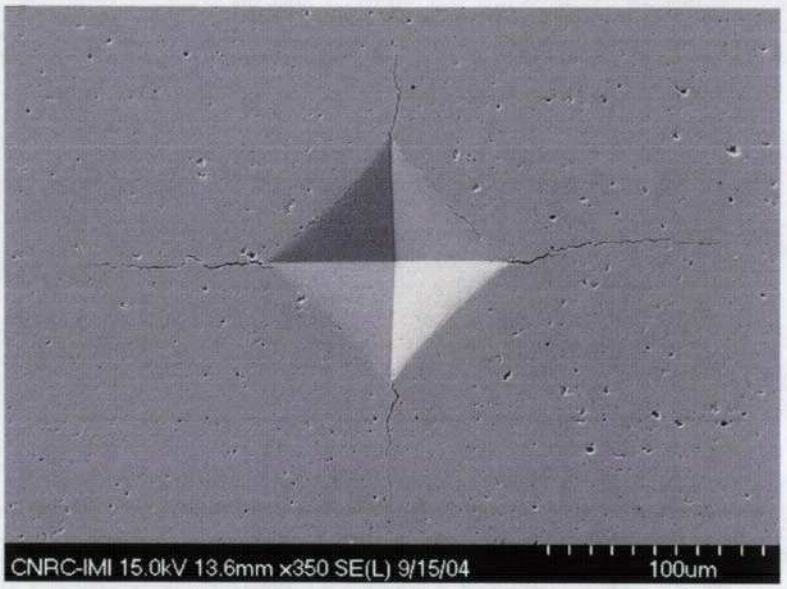

(a)

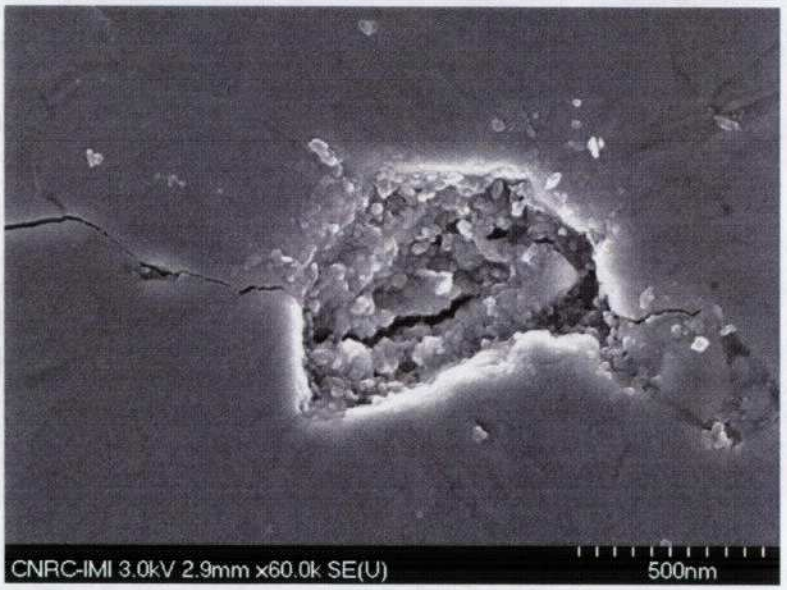

(b)

Figure 8 – (a) Vickers indentation impression (5 kgf) and crack propagation in the cross-section of the HVOF-sprayed titania coating made from the nanostructured feedstock (Fig. 1). (b) Vickers indentation crack tip arresting after passing through a nanozone in the nanostructured coating [10].

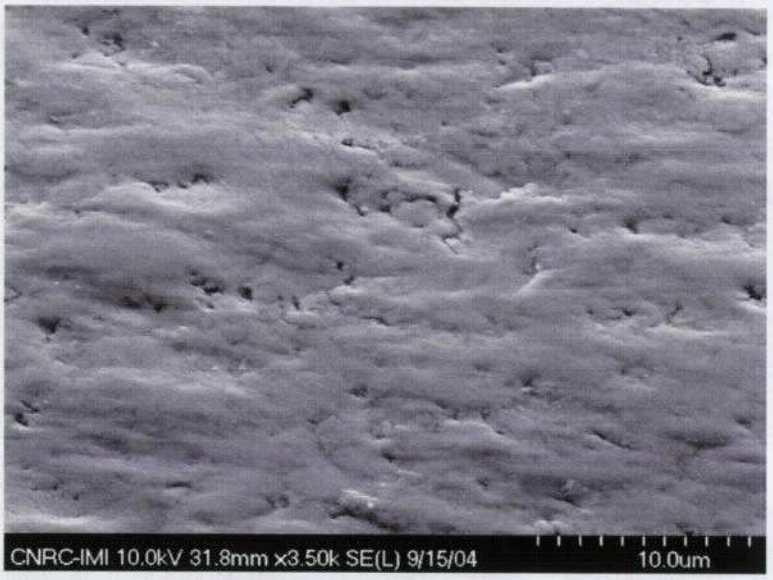

Figure 9 – SEM picture (taken at 50° angle) of the wear scar of an HVOF-sprayed nanostructured titania coating of Figs. 6 and 8 [10].

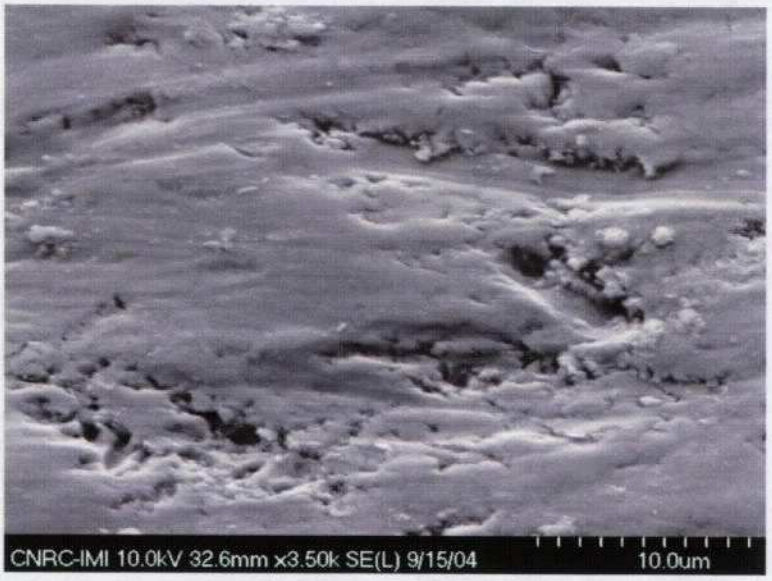

Figure 10 – SEM picture (taken at 50° angle) of the wear scar of an HVOF-sprayed conventional titania coating of Figs. 5 and 7 [10].

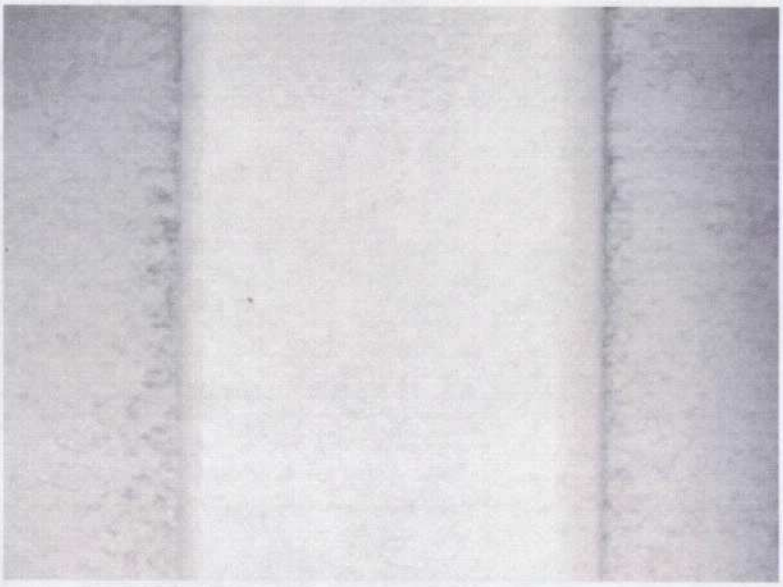

Figure 11 – Wear scar formed during rub-rig testing on the surface of nanostructured YSZ coating of Fig. 4 [40].

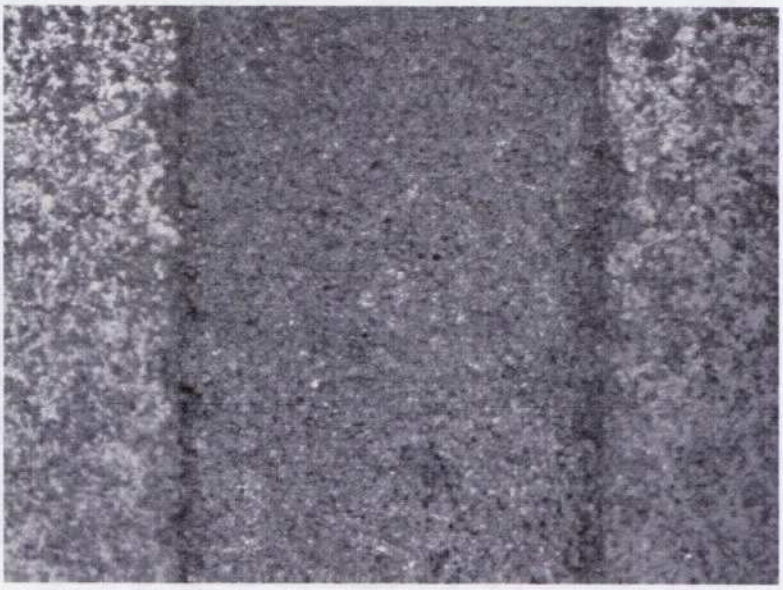

Figure 12 – Wear scar formed during rub-rig testing on the surface of CoNiCrAlY-BN-polyester abradable coating.

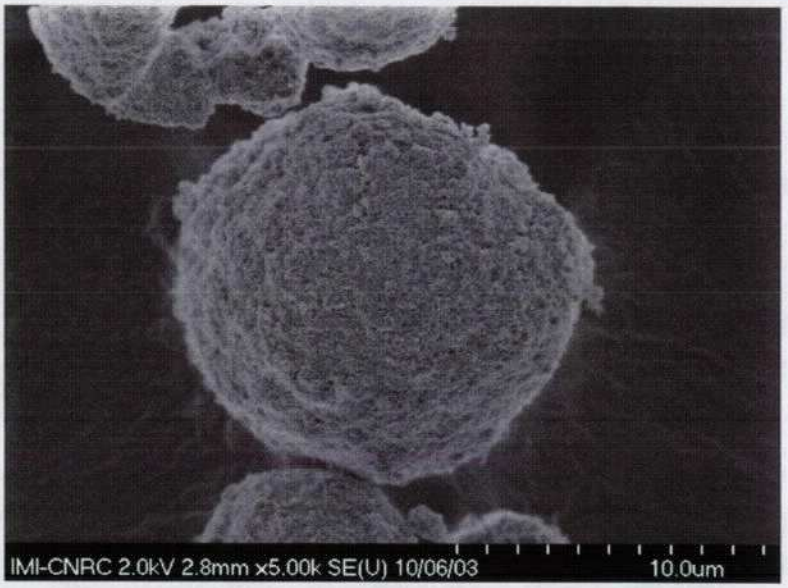

(a)

(b)

Figure 13 – (a) HA feedstock particle formed by the agglomeration (spray-drying) of individual nanosized particles of HA. (b) Particle of (a) observed at higher magnification; individual nanosized HA particles with widths smaller than 100 nm.

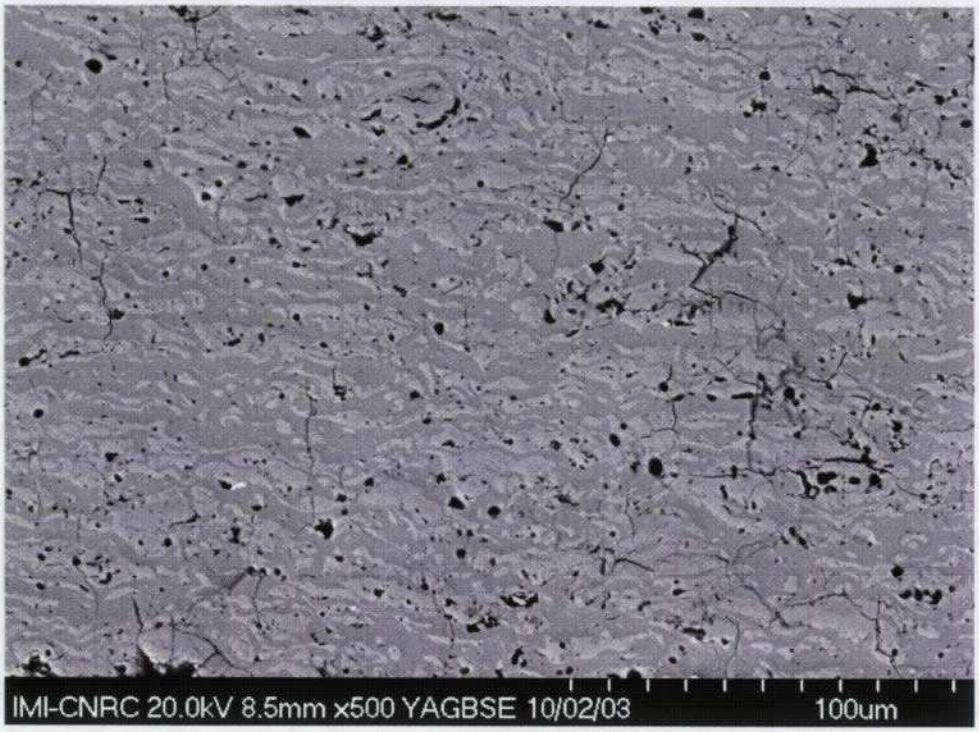

Figure 14 – Cross-section of an HVOF-sprayed HA coating made from a nanostructured feedstock (Fig. 13) [15].

(a)

(b)

(c)

Figure 15 – Different types of nanostructural characteristics found in the cross-section of the HVOF-sprayed nano HA coating of Fig. 14. (a) porous, (b) fibrous [15] and (c) densely packed [15] nanozones.

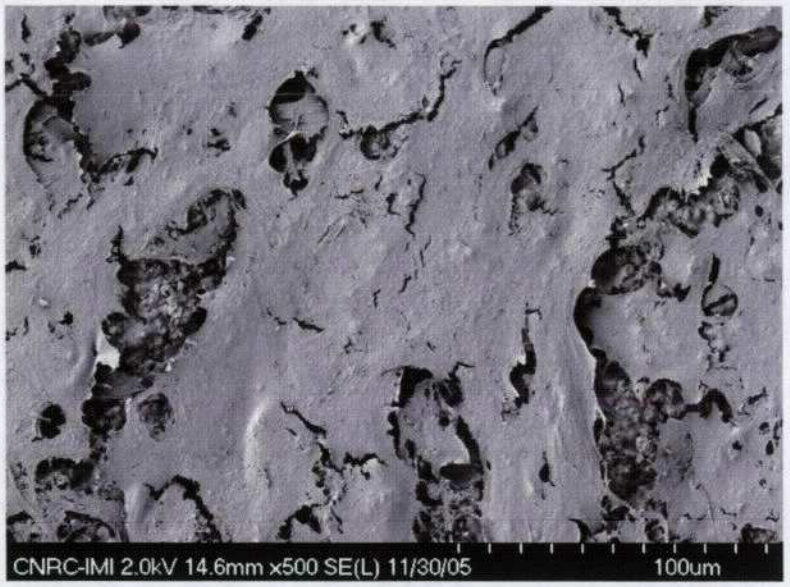

Figure 16 – Osteoblast cell culture (7 day-incubation) on the surface of the HVOF-sprayed nano TiO_2 coating of Figs. 6 and 8.

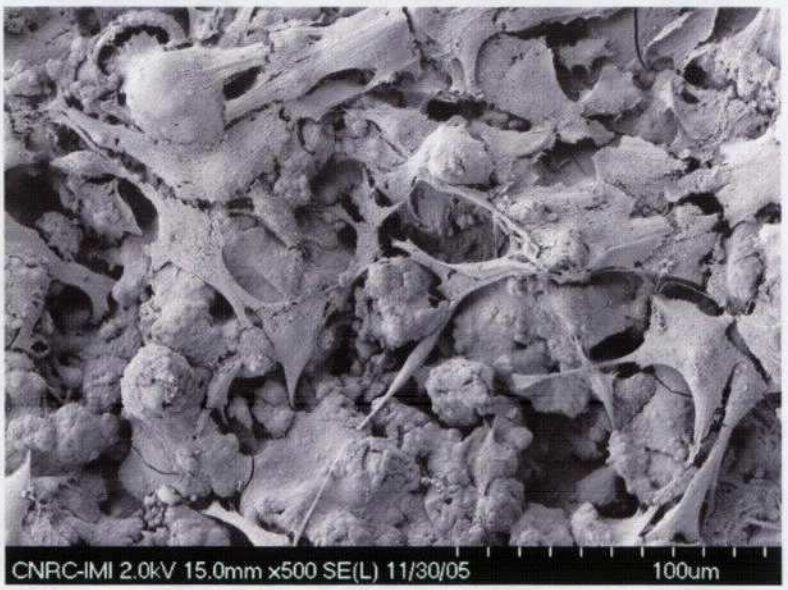

Figure 17 – Osteoblast cell culture (7 day-incubation) on the surface of an APS conventional HA coating.

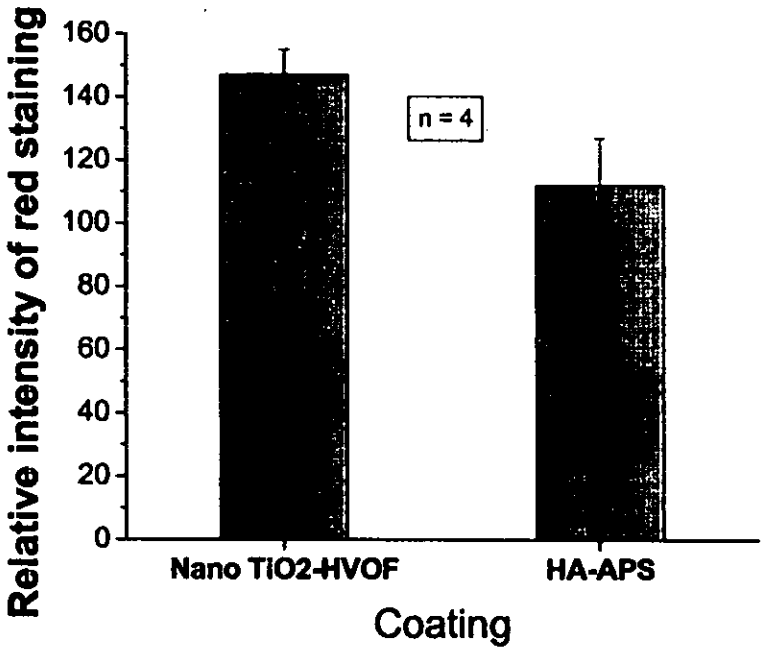

Figure 18 - Relative intensity of red staining (alkaline phosphatase activity) for the osteoblast cells on the surface of the HVOF-sprayed nano TiO_2 (Figs. 6 and 8) and APS conventional HA (Fig. 16) coatings after a 15-day cell culture. The percentage of the coating covered in red is a measure of the osteoblast cells' ability to adhere, proliferate, and differentiate on the coating surface.

(a)

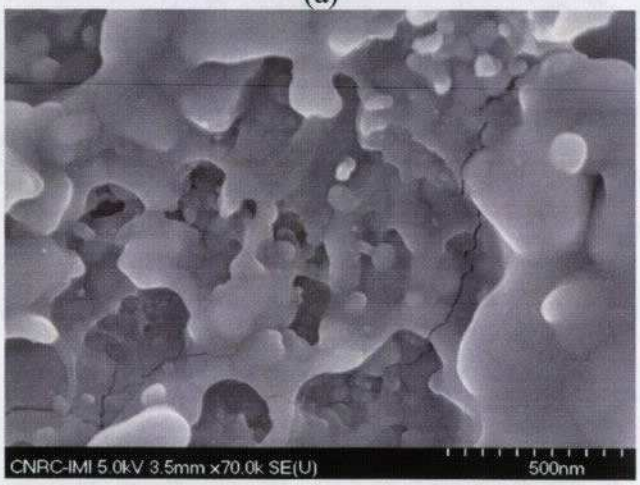

(b)

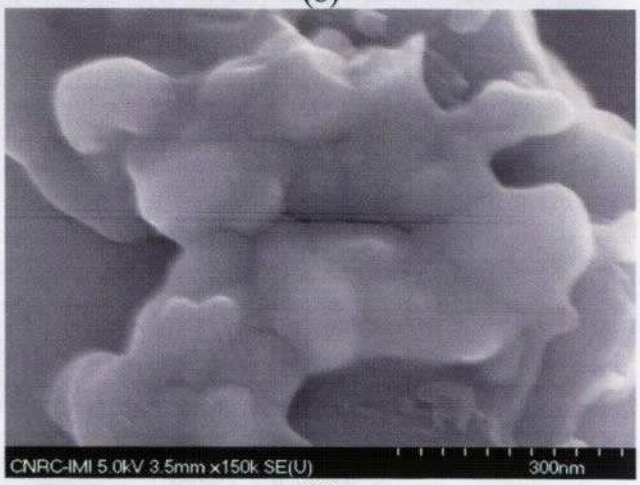

(c)

Figure 19 – (a) (b) (c) Images of nanozones found on the as-sprayed surface of the HVOF-sprayed nano titania coating of Figs. 6 and 8.